Numerical implementation and assessment of the GLPD micromorphic model of ductile rupture

Koffi Enakoutsa and Jean-Baptiste Leblond

UPMC Univ Paris 06, UMR 7190, Institut Jean Le Rond d'Alembert, Tour 65-55, 4 place Jussieu, 75005 Paris, France

Abstract

Just like all constitutive models involving softening, Gurson's classical model for porous ductile solids predicts unrealistic, unlimited localization of strain and damage. An improved variant of this model aimed at solving this problem has been proposed by Gologanu, Leblond, Perrin and Devaux (GLPD) on the basis of some refinement of Gurson's original homogenization procedure. The GLPD model is of "micromorphic" nature since it involves the second gradient of the macroscopic velocity and generalized macroscopic stresses of "moment" type. This work is devoted to the numerical implementation and the assessment of the practical relevance of this new model. This assessment is based on two criteria: absence of mesh size effects in finite element computations and agreement of numerical and experimental results for some typical experiments of ductile fracture. The GLPD model is found to pass both tests. It is therefore concluded that it represents a viable, although admittedly complex solution to the problem of unlimited localization in Gurson's model of ductile rupture.

Key words: Ductile rupture, Gurson's model, unlimited localization, micromorphic model, numerical simulations

1 Introduction

Constitutive models involving softening all predict unlimited localization of strain and damage. This feature generates such undesired phenomena as absence of energy dissipation during crack propagation and mesh size sensitivity in finite element computations. Gurson (1977)'s famous model for porous ductile materials, which was derived from approximate limit-analysis of some elementary voided cell in a plastic solid, is no exception. In this model, unlimited localization arises from the softening due to the gradual increase of the porosity.

Several proposals have been made to solve this problem. One of these, due to Leblond *et al.* (1994) but based on a previous suggestion made by Pijaudier-Cabot and Bazant (1987) in the context of damage of concrete, consists of adopting a nonlocal evolution equation for the porosity involving some spatial convolution of some "local porosity rate" within

an otherwise unmodified Gurson model. This simple proposal has attracted the attention of several authors (Tvergaard and Needleman (1995), Tvergaard and Needleman (1997), Needleman and Tvergaard (1998), Enakoutsa *et al.* (2007)). It was notably checked by Tvergaard and Needleman (1995) that it indeed allows to eliminate mesh size effects. Also, Enakoutsa *et al.* (2007) showed that with a minor modification, it leads to very good numerical reproduction of the results of typical experiments of ductile rupture.

One shortcoming of Leblond *et al.* (1994)'s proposal, however, is that it is purely heuristic and lacks any serious theoretical justification. This was the motivation for a later, more elaborate and physically-based proposal of Gologanu *et al.* (1997). These authors derived an improved variant of Gurson's model (the *GLPD model*[1]) through some refinement of this author's original homogenization procedure based on Mandel (1964)'s and Hill (1967)'s classical conditions of homogeneous boundary strain rate. In the approach of Gologanu *et al.* (1997), the boundary velocity is assumed to be a quadratic, rather than linear, function of the coordinates. The physical idea is to approximately account in this way for the possibility of quick variations of the macroscopic strain rate, such as encountered during strain localization, over short distances of the order of the size of the elementary cell considered. The output of the homogenization procedure is a model of "micromorphic" nature involving the second gradient of the macroscopic velocity and generalized macroscopic stresses of "moment" type (homogeneous to the product of a stress and a distance).

The aim of this paper is to critically assess the practical relevance of the GLPD model through implementation into some finite element (FE) code and study of its numerical predictions. The assessment will be based on two criteria. First, numerical computations using the new model must no longer exhibit any pathological dependence upon the mesh size. Second, it must be able to satisfactorily reproduce the results of typical experiments of ductile rupture.

The paper is organized as follows:

- Section 2 provides a summary of the equations of the GLPD model. The micromechanical foundations of these equations are recalled for completeness in Appendix A.
- Section 3 discusses the numerical implementation of the model into some FE programme. The main difficulty encountered here relates to the necessary operation of "projection" of the elastic stress predictor onto the sophisticated GLPD yield locus. This operation is achieved through some adaptation of Nguyen (1977)'s classical implicit (backward Euler) algorithm for projection onto the von Mises yield locus. The advantage of this algorithm is that for models such as that envisaged here, which fit into the framework of *generalized standard materials* (Halphen and Nguyen (1975)), it warrants existence and uniqueness of the solution of the projection problem. This problem is reduced to the search for the values of two scalar unknowns through some suitable parametrization of the GLPD yield locus.
- Section 4 then provides an analytic solution of the equations of the model for the circular bending of a beam in plane strain, in the limiting case of a zero porosity. This solution is used to assess the programme developed. It is also intrinsically interesting in that

[1] GLPD: Gologanu-Leblond-Perrin-Devaux.

it allows to check that the predictions of the GLPD model do correspond to what its micromechanical foundations suggest they should be in the specific case considered.
- Finally Section 5 is devoted to numerical applications. The question of mesh size effects is envisaged first through consideration of a convenient imaginary pre-notched specimen. Numerical results clearly show the difference between the original Gurson model, which does exhibit an influence of mesh size upon the load-displacement curve in the softening region, and the GLPD model, which does not. The ability of the GLPD model to numerically reproduce the results of actual experiments of ductile fracture is examined next through consideration of tests performed on typical axisymmetric pre-cracked specimens. The agreement between the experimental and numerical load-displacement curves is found to be quite acceptable even in the softening region.

2 The GLPD micromorphic model for porous ductile solids

Since the original reference (Gologanu *et al.* (1997)) for the GLPD model is not easily accessible, a summary of the equations of this model is given here. A short presentation of the derivation of these equations from some homogenization procedure is also provided in Appendix A; strictly speaking, this presentation is not indispensable, but it is useful to fully grasp the physical foundations of the model.

2.1 Generalities

In the GLPD model, internal forces are represented through some ordinary second-rank symmetric Cauchy stress tensor $\mathbf{\Sigma}$ plus some additional third-rank "moment tensor" $\mathbf{M}$ symmetric in its first two indices only [2]. The components of $\mathbf{M}$ are related through the three conditions

$$M_{ijj} = 0. \tag{1}$$

(These conditions may be compared to the condition of plane stress in the theory of thin plates or shells).

The virtual power of internal forces is given by the expression

$$\mathcal{P}^{(i)} \equiv -\int_\Omega (\mathbf{\Sigma} : \mathbf{D} + \mathbf{M} \vdots \nabla\mathbf{D})\, d\Omega \tag{2}$$

where Ω denotes the domain considered, $\mathbf{D} \equiv \frac{1}{2}\left[\nabla\mathbf{V} + (\nabla\mathbf{V})^T\right]$ ($\mathbf{V}$: material velocity) the Eulerian strain rate, $\nabla\mathbf{D}$ its gradient, $\mathbf{\Sigma} : \mathbf{D}$ the double inner product $\Sigma_{ij}D_{ij}$ and $\mathbf{M} \vdots \nabla\mathbf{D}$ the triple inner product $M_{ijk}D_{ij,k}$.

[2] The component M_{ijk} is noted $M_{k|ij}$ in Gologanu *et al.* (1997)'s original paper. The present notation leads to more natural-looking expressions.

The virtual power of external forces is given by

$$\mathcal{P}^{(e)} \equiv \int_{\partial\Omega} \mathbf{T}.\mathbf{V}\, dS \tag{3}$$

where $\mathbf{T}$ represents some surface traction [3].

The hypothesis of additivity of elastic and plastic strain rates reads

$$\begin{cases} \mathbf{D} & \equiv \mathbf{D}^e + \mathbf{D}^p \\ \nabla\mathbf{D} & \equiv (\nabla\mathbf{D})^e + (\nabla\mathbf{D})^p. \end{cases} \tag{4}$$

The elastic and plastic parts $(\nabla\mathbf{D})^e$, $(\nabla\mathbf{D})^p$ of the gradient of the strain rate here do *not* coincide in general with the gradients $\nabla(\mathbf{D}^e)$, $\nabla(\mathbf{D}^p)$ of the elastic and plastic parts of the strain rate.

2.2 Hypoelasticity law

The elastic parts of the strain rate and its gradient are related to the rates of the stress and moment tensors through the following hypoelasticity law:

$$\begin{cases} \dfrac{D\Sigma_{ij}}{Dt} & = \lambda\,\delta_{ij} D^e_{kk} + 2\mu D^e_{ij} \\ \dfrac{DM_{ijk}}{Dt} & = \dfrac{b^2}{5}\left[\lambda\,\delta_{ij}(\nabla D)^e_{hhk} + 2\mu(\nabla D)^e_{ijk} - 2\lambda\,\delta_{ij}U^e_k - 2\mu\left(\delta_{ik}U^e_j + \delta_{jk}U^e_i\right)\right]. \end{cases} \tag{5}$$

In these expressions λ and μ denote the Lamé coefficients and b the mean half-spacing between neighboring voids [4]. Also, $\frac{D\Sigma_{ij}}{Dt}$ and $\frac{DM_{ijk}}{Dt}$ are the Jaumann (objective) time-derivatives of Σ_{ij} and M_{ijk}, given by

$$\begin{cases} \dfrac{D\Sigma_{ij}}{Dt} & \equiv \dot{\Sigma}_{ij} + \Omega_{ki}\Sigma_{kj} + \Omega_{kj}\Sigma_{ik} \\ \dfrac{DM_{ijk}}{Dt} & \equiv \dot{M}_{ijk} + \Omega_{hi}M_{hjk} + \Omega_{hj}M_{ihk} + \Omega_{hk}M_{ijh} \end{cases} \tag{6}$$

where $\mathbf{\Omega} \equiv \frac{1}{2}\left[\nabla\mathbf{V} - (\nabla\mathbf{V})^T\right]$ is the antisymmetric part of the velocity gradient. Finally $\mathbf{U}^e$ is a vector the value of which is fixed by equations (1) (written in rate form, $\frac{DM_{ijj}}{Dt} = 0$):

$$U^e_i = \frac{\lambda(\nabla D)^e_{hhi} + 2\mu(\nabla D)^e_{ihh}}{2\lambda + 8\mu}. \tag{7}$$

(This vector may be compared to the through-the-thickness component of the elastic strain rate in the theory of thin plates or shells, the value of which is fixed by the condition of plane stress).

[3] The general equilibrium equations and boundary conditions corresponding to the expressions (2) and (3) of the virtual powers of internal and external forces need not be given since they are not necessary for the numerical implementation.

[4] In the homogenization procedure, this is the radius of the spherical elementary cell considered.

2.3 Yield criterion

The plastic behavior is governed by the following Gurson-like criterion:

$$\Phi(\boldsymbol{\Sigma}, \mathbf{M}) \equiv \frac{1}{\Sigma^2}\left(\Sigma_{eq}^2 + \frac{Q^2}{b^2}\right) + 2p\,\cosh\left(\frac{3}{2}\frac{\Sigma_m}{\Sigma}\right) - 1 - p^2 \leq 0. \tag{8}$$

In this expression:

- $\Sigma_{eq} \equiv \left(\frac{3}{2}\boldsymbol{\Sigma}' : \boldsymbol{\Sigma}'\right)^{1/2}$ ($\boldsymbol{\Sigma}'$: deviator of $\boldsymbol{\Sigma}$) is the von Mises equivalent stress.
- $\Sigma_m \equiv \frac{1}{3}\,\mathrm{tr}\,\boldsymbol{\Sigma}$ is the mean stress.
- Σ represents a kind of average value of the yield stress in the heterogeneous metallic matrix, the evolution equation of which is given below.
- p is a parameter connected to the porosity (void volume fraction) f through the relation:

$$p \equiv q f^* \quad , \quad f^* \equiv \begin{cases} f & \text{if} \quad f \leq f_c \\ f_c + \delta(f - f_c) & \text{if} \quad f > f_c \end{cases} \tag{9}$$

  where q is *Tvergaard's parameter*, f_c the *critical porosity at the onset of coalescence of voids*, and δ (> 1) a factor describing the accelerated degradation of the material during coalescence (Tvergaard (1981), Tvergaard and Needleman (1984)).
- Q^2 is a quadratic form of the components of the moment tensor given by

$$Q^2 \equiv A_1\mathcal{M}_1 + A_2\mathcal{M}_2 \quad , \quad \begin{cases} A_1 = 0.194 \\ A_2 = 6.108 \end{cases} \tag{10}$$

  where $\mathcal{M}_1$ and $\mathcal{M}_2$ are the quadratic invariants of $\mathbf{M}$ defined by:

$$\begin{cases} \mathcal{M}_1 \equiv M_{mi}M_{mi} \\ \mathcal{M}_2 \equiv \frac{3}{2}M'_{ijk}M'_{ijk}, \end{cases} \tag{11}$$

  $M_{mi} \equiv \frac{1}{3}M_{hhi}$ and $\mathbf{M}'$ denoting the mean and deviatoric parts of $\mathbf{M}$, taken over its first two indices.

2.4 Flow rule

The plastic parts of the strain rate and its gradient are given by the flow rule associated to the criterion (8) through normality:

$$\begin{cases} D^p_{ij} & = H\dfrac{\partial\Phi}{\partial\Sigma_{ij}}(\boldsymbol{\Sigma}, \mathbf{M}) \\ (\nabla D)^p_{ijk} & = H\dfrac{\partial\Phi}{\partial M_{ijk}}(\boldsymbol{\Sigma}, \mathbf{M}) + \delta_{ik}U^p_j + \delta_{jk}U^p_i \end{cases} \quad , \quad H \begin{cases} = 0 & \text{if} \quad \Phi(\boldsymbol{\Sigma}, \mathbf{M}) < 0 \\ \geq 0 & \text{if} \quad \Phi(\boldsymbol{\Sigma}, \mathbf{M}) = 0. \end{cases} \tag{12}$$

The term $\delta_{ik}U_j^p + \delta_{jk}U_i^p$ in equation $(12)_2$ represents a rigid-body motion of the elementary cell, which is left unspecified by the flow rule but fixed in practice by conditions (1). (The vector $\mathbf{U}^p$ may be compared to the through-the-thickness component of the plastic strain rate in the theory of thin plates or shells, the value of which is fixed by the condition of plane stress).

The values of the derivatives of the yield function $\Phi(\mathbf{\Sigma}, \mathbf{M})$ in equations (12) are readily calculated to be

$$\left\{ \begin{array}{l} \dfrac{\partial \Phi}{\partial \Sigma_{ij}} = 3\dfrac{\Sigma'_{ij}}{\Sigma^2} + \dfrac{p}{\Sigma}\,\delta_{ij}\sinh\left(\dfrac{3}{2}\dfrac{\Sigma_m}{\Sigma}\right) \\ \dfrac{\partial \Phi}{\partial M_{ijk}} = \dfrac{1}{\Sigma^2 b^2}\left(\dfrac{2}{3}A_1\delta_{ij}M_{mk} + 3A_2 M'_{ijk}\right). \end{array} \right. \tag{13}$$

2.5 Evolution of internal parameters

The evolution of the porosity is governed by the classical equation resulting from approximate incompressibility of the metallic matrix:

$$\dot{f} = (1-f)\,\mathrm{tr}\,\mathbf{D}^p. \tag{14}$$

The parameter Σ is given by

$$\Sigma \equiv \sigma(E) \tag{15}$$

where $\sigma(\epsilon)$ is the function which provides the yield stress of the matrix material in terms of the local equivalent cumulated plastic strain ϵ, and E represents some average value of this equivalent strain in the heterogeneous matrix. The evolution of E is governed by the following equation:

$$(1-f)\Sigma\dot{E} = \mathbf{\Sigma} : \mathbf{D}^p + \mathbf{M} \vdots (\nabla \mathbf{D})^p. \tag{16}$$

3 Numerical implementation

The GLPD model described in Section 2 has been incorporated into the SYSTUS® FE code developed by ESI Group, in the 2D case. The trickiest features of the numerical implementation, which stands as an extension of those proposed by Aravas (1987) and Enakoutsa *et al.* (2007) for the original Gurson model, are presented here. Emphasis is mainly placed on the complex problem of projection of the (supposedly known) elastic stress predictor onto the yield locus defined by the yield function (8). (This problem will simply be called the *projection problem* for shortness in the sequel).

3.1 The GLPD model and the class of generalized standard materials

The class of *generalized standard materials*, as defined by Halphen and Nguyen (1975), consists of elastic-plastic materials for which the plastic strain *plus* the internal parameters

collectively obey some "extended normality rule". This class is remarkable in that as shown by Nguyen (1977), for such materials, provided that the flow rule is discretized in time with an *implicit* (backward Euler) scheme, the projection problem is equivalent to minimizing some strictly convex function, which warrants existence and uniqueness of its solution.

It so happens that the GLPD model fits into the framework of generalized standard materials *for a fixed porosity*. This property is tied to the special evolution equation (16) obeyed by the hardening parameter E. The proof is provided in Enakoutsa's thesis (Enakoutsa (2007)) and is in fact a straightforward extension of that given by Enakoutsa *et al.* (2007) for the original Gurson model.

This property strongly suggests to adopt an *implicit* algorithm to solve the projection problem, in order to take advantage of the guaranteed existence and uniqueness of the solution. However, since the porosity f must not be allowed to vary for the GLPD model to be "generalized standard", it appears necessary, in order to benefit from this property, to exceptionally use an *explicit* scheme with respect to this specific parameter. Then f will be fixed during the whole calculation of the values of field quantities at time $t + \Delta t$ from their values at time t, and updated (using a discretized version of equation (14)) only at the very end upon convergence; the projection algorithm will then be exactly the same *as if* the porosity were a constant.

We shall therefore use the explicit estimate of the porosity at time $t + \Delta t$ given by

$$f(t + \Delta t) \simeq f(t) + \dot{f}(t)\Delta t, \tag{17}$$

and the explicit estimate of the parameter $p(t + \Delta t)$ resulting from there, during the whole "transition from time t to time $t+\Delta t$", but the projection algorithm developed will otherwise be fully implicit with respect to all other parameters, that is the components of the plastic strain and the plastic strain gradient and the hardening parameter E.

From now on, all quantities will implicitly be considered at time $t + \Delta t$.

3.2 Parametrization of the yield locus

One key point of the procedure of solution of the projection problem, aimed at reducing the number of unknowns, lies in a suitable partial parametrization of the yield locus defined by the yield function (8). This parametrization is inspired from the classical one for an ellipse and obtained by looking for the maximum possible value of the quantity $\Sigma_{eq}^2 + Q^2/b^2$, namely $(1-p)^2\Sigma^2$, and then writing this quantity in the form $(1-p)^2\,\Sigma^2\cos^2\phi$ for some angle ϕ and solving the equation $\Phi(\boldsymbol{\Sigma}, \mathbf{M}) = 0$ with respect to Σ_m. One thus gets

$$\begin{cases} \Sigma_{eq}^2 + \dfrac{Q^2}{b^2} \equiv (1-p)^2\,\Sigma^2\cos^2\phi & \\ \Sigma_m \equiv \dfrac{2}{3}\,\Sigma\,\mathrm{sgn}(\phi)\,\mathrm{arg\,cosh}\left[1 + \dfrac{(1-p)^2\sin^2\phi}{2p}\right] & , \quad \phi \in \left[-\dfrac{\pi}{2}, \dfrac{\pi}{2}\right]. \end{cases} \tag{18}$$

The sign of the parameter ϕ is introduced into equation $(18)_2$ in order to allow for negative as well as positive values of Σ_m.

This parametrization is only partial since it does not specify the values of the unknowns Σ_{eq}^2 and Q^2 separately but only that of the sum $\Sigma_{eq}^2 + Q^2/b^2$.

3.3 Solution of the projection problem for a fixed hardening parameter

Momentarily assuming the value of the current yield stress Σ to be known, we shall now show how the projection problem can be solved through combination of the yield criterion and the flow rule. This problem will be reduced to a system of two coupled equations on the unknowns ϕ and Σ_{eq}, to be solved numerically.

The flow rule (12) will be rewritten by distinguishing the mean $(_m)$ and deviatoric $(')$ parts of the various tensors, the mean and deviatoric parts of a third-rank tensor symmetric in its first two indices being taken over these indices as above. The flow rule reads then in time-discretized form:

$$\begin{cases} (\Delta E)^{p\,\prime}_{ij} &= \dfrac{3}{2}\dfrac{(\Delta E)^p_{eq}}{\Sigma_{eq}}\Sigma'_{ij} \\ (\Delta E)^p_m &= \dfrac{p}{2}\dfrac{\Sigma}{\Sigma_{eq}}\sinh\left(\dfrac{3}{2}\dfrac{\Sigma_m}{\Sigma}\right)(\Delta E)^p_{eq} \\ (\nabla\Delta E)^{p\,\prime}_{ijk} &= \dfrac{(\Delta E)^p_{eq}}{2b^2}\left(3\dfrac{A_2}{\Sigma_{eq}}M'_{ijk} + \delta_{ik}U^p_j + \delta_{jk}U^p_i - \dfrac{2}{3}\delta_{ij}U^p_k\right) \\ (\nabla\Delta E)^p_{mk} &= \dfrac{(\Delta E)^p_{eq}}{3b^2}\left(\dfrac{A_1}{\Sigma_{eq}}M_{mk} + U^p_k\right). \end{cases} \tag{19}$$

In these equations the plastic parts of the strain rate and its gradient $\mathbf{D}^p$, $(\nabla\mathbf{D})^p$ have been replaced by the plastic parts of the increment of strain and its gradient $(\Delta\mathbf{E})^p$, $(\nabla\Delta\mathbf{E})^p$, and the plastic multiplier H has been re-expressed in terms of the equivalent increment of plastic strain $(\Delta E)^p_{eq}$. Also, the definition of the arbitrary vector $\mathbf{U}^p$ has been modified by a multiplicative constant in order to simplify future expressions.

Note that the numerical scheme leading from the theoretical flow rule (12) to its discrete counterpart (19) is implicit, as announced, since the stress and moment components and the yield stress are taken at time $t + \Delta t$ in the right-hand side of equations (19).

Let ${\Sigma'_{ij}}^*$, ${\Sigma_m}^*$, ${M'_{ijk}}^*$, ${M_{mk}}^*$ denote the elastic predictors of the quantities Σ'_{ij}, Σ_m, M'_{ijk} and M_{mk}, that is their virtual (supposedly known) values at time $t + \Delta t$ obtained from those at time t by imagining the increments of strain and its gradient to be purely elastic. (These elastic predictors include the terms proportional to $\mathbf{\Omega}$ in the expressions (6) of the Jaumann derivatives of $\mathbf{\Sigma}$ and $\mathbf{M}$). By the hypoelasticity law (5), the true values at time

$t + \Delta t$ are related to their elastic predictors by the relations

$$\begin{cases} \Sigma'_{ij} &= {\Sigma'_{ij}}^* - 2\mu(\Delta E)^{p\,\prime}_{ij} \\ \Sigma_m &= {\Sigma_m}^* - (3\lambda + 2\mu)(\Delta E)^p_m \\ M'_{ijk} &= {M'_{ijk}}^* - 2\mu\dfrac{b^2}{5}(\nabla\Delta E)^{p\,\prime}_{ijk} \\ M_{mk} &= {M_{mk}}^* - (3\lambda + 2\mu)\dfrac{b^2}{5}(\nabla\Delta E)^p_{mk}. \end{cases} \tag{20}$$

Equations $(20)_3$ and $(20)_4$ here have been obtained by omitting the terms involving the vector $\mathbf{U}^e$ in the hypoelasticity law $(5)_2$. This is permissible since the sole role of this vector is to ensure satisfaction of equations (1), and the job will be done by the vector $\mathbf{U}^p$ anyway.

It is now necessary to separately combine equations $(19)_1$ and $(20)_1$, $(19)_2$ and $(20)_2$, $(19)_3$ and $(20)_3$, $(19)_4$ and $(20)_4$.

- *Equations $(19)_1$ and $(20)_1$* imply that

$$\Sigma'_{ij} = {\Sigma'_{ij}}^* - 3\mu\frac{(\Delta E)^p_{eq}}{\Sigma_{eq}}\Sigma'_{ij} \quad \Rightarrow \quad \left[1 + 3\mu\frac{(\Delta E)^p_{eq}}{\Sigma_{eq}}\right]\Sigma'_{ij} = {\Sigma'_{ij}}^*.$$

  This relation bears two consequences. First, the tensors $\mathbf{\Sigma}'$ and $\mathbf{\Sigma}'^*$ are positively collinear so that

$$\Sigma'_{ij} = \frac{\Sigma_{eq}}{{\Sigma_{eq}}^*}{\Sigma'_{ij}}^* \tag{21}$$

  where ${\Sigma_{eq}}^*$ denotes the von Mises norm (equivalent stress) of the elastic predictor $\mathbf{\Sigma}'^*$. Second, taking the von Mises norms of both sides, one gets

$$(\Delta E)^p_{eq} = \frac{{\Sigma_{eq}}^* - \Sigma_{eq}}{3\mu}. \tag{22}$$

- *Equations $(19)_2$ and $(20)_2$* imply that

$$\Sigma_m = {\Sigma_m}^* - (3\lambda + 2\mu)\frac{p}{2}\frac{\Sigma}{\Sigma_{eq}}\sinh\left(\frac{3}{2}\frac{\Sigma_m}{\Sigma}\right)(\Delta E)^p_{eq}.$$

  Combining this result with equation (22), one gets the relation

$$\boxed{\left[\frac{6\mu}{3\lambda + 2\mu}({\Sigma_m}^* - \Sigma_m) + p\,\Sigma\,\sinh\left(\frac{3}{2}\frac{\Sigma_m}{\Sigma}\right)\right]\Sigma_{eq} = p\,\Sigma\,{\Sigma_{eq}}^*\,\sinh\left(\frac{3}{2}\frac{\Sigma_m}{\Sigma}\right).} \tag{23}$$

  This is the first equation of the system looked for on the unknowns ϕ and Σ_{eq}. The left-hand side depends on both ϕ (through the expression $(18)_2$ of Σ_m) and Σ_{eq} while the right-hand side depends only on ϕ.
- *Equations $(19)_3$ and $(20)_3$* imply that

$$M'_{ijk} = {M'_{ijk}}^* - \frac{\mu}{5}(\Delta E)^p_{eq}\left(3\frac{A_2}{\Sigma_{eq}}M'_{ijk} + \delta_{ik}U^p_j + \delta_{jk}U^p_i - \frac{2}{3}\delta_{ij}U^p_k\right).$$

Using equation (22), this relation may be re-written in the form

$$\left(1+\frac{A_2}{5}\frac{{\Sigma_{eq}}^*-\Sigma_{eq}}{\Sigma_{eq}}\right)M'_{ijk}={M'_{ijk}}^{**} \tag{24}$$

where

$${M'_{ijk}}^{**}\equiv {M'_{ijk}}^{*}-\frac{{\Sigma_{eq}}^*-\Sigma_{eq}}{15}\left(\delta_{ik}U^p_j+\delta_{jk}U^p_i-\frac{2}{3}\delta_{ij}U^p_k\right). \tag{25}$$

(Note that in contrast to the elastic predictor $\mathbf{M}'^{*}$, the tensor $\mathbf{M}'^{**}$ defined by (25) is not known *a priori* since both Σ_{eq} and $\mathbf{U}^p$ are unknown). The consequences of equation (24) are twofold. First, it implies that the tensors $\mathbf{M}'$ and $\mathbf{M}'^{**}$ are positively collinear so that

$$M'_{ijk}=\sqrt{\frac{\mathcal{M}_2}{{\mathcal{M}_2}^{**}}}\;{M'_{ijk}}^{**} \tag{26}$$

where $\mathcal{M}_2$ and ${\mathcal{M}_2}^{**}$ are the quadratic invariants of $\mathbf{M}'$ and $\mathbf{M}'^{**}$ defined by equation $(11)_2$. Second, taking the "$\mathcal{M}_2$ invariants" of both sides, one gets

$$\mathcal{M}_2=\left[\frac{\Sigma_{eq}}{\Sigma_{eq}+\frac{A_2}{5}\left({\Sigma_{eq}}^*-\Sigma_{eq}\right)}\right]^2{\mathcal{M}_2}^{**}. \tag{27}$$

- *Equations $(19)_4$ and $(20)_4$* finally imply that

$$M_{mk}={M_{mk}}^{*}-\frac{3\lambda+2\mu}{15}(\Delta E)^p_{eq}\left(\frac{A_1}{\Sigma_{eq}}M_{mk}+U^p_k\right).$$

Combination with equation (22) yields

$$\left(1+\frac{3\lambda+2\mu}{45\mu}A_1\frac{{\Sigma_{eq}}^*-\Sigma_{eq}}{\Sigma_{eq}}\right)M_{mk}={M_{mk}}^{**} \tag{28}$$

where

$${M_{mk}}^{**}\equiv {M_{mk}}^{*}-\frac{3\lambda+2\mu}{45\mu}\left({\Sigma_{eq}}^*-\Sigma_{eq}\right)U^p_k. \tag{29}$$

(Again, the vector ${\mathbf{M}_m}^{**}$ defined by (29) is not known *a priori* since Σ_{eq} and $\mathbf{U}^p$ are unknown). Equation (28) again bears two consequences. First, the vectors $\mathbf{M}_m$ and ${\mathbf{M}_m}^{**}$ are positively collinear so that

$$M_{mk}=\sqrt{\frac{\mathcal{M}_1}{{\mathcal{M}_1}^{**}}}\;{M_{mk}}^{**} \tag{30}$$

where $\mathcal{M}_1$ and ${\mathcal{M}_1}^{**}$ are the quadratic invariants of $\mathbf{M}_m$ and ${\mathbf{M}_m}^{**}$ defined by equation $(11)_1$. Second, taking the "$\mathcal{M}_1$ invariants" of both sides, one gets

$$\mathcal{M}_1=\left[\frac{\Sigma_{eq}}{\Sigma_{eq}+\frac{3\lambda+2\mu}{45\mu}A_1\left({\Sigma_{eq}}^*-\Sigma_{eq}\right)}\right]^2{\mathcal{M}_1}^{**}. \tag{31}$$

We shall now combine these results with equation (1) in order to express the vector $\mathbf{U}^p$ in terms of the sole unknown Σ_{eq}. First, using equations (24) and (25), one gets

$$M'_{ijk}=\frac{\Sigma_{eq}}{\Sigma_{eq}+\frac{A_2}{5}\left({\Sigma_{eq}}^*-\Sigma_{eq}\right)}\left[{M'_{ijk}}^{*}-\frac{{\Sigma_{eq}}^*-\Sigma_{eq}}{15}\left(\delta_{ik}U^p_j+\delta_{jk}U^p_i-\frac{2}{3}\delta_{ij}U^p_k\right)\right].$$

Combination of equations (28) and (29) also yields

$$M_{mk} = \frac{\Sigma_{eq}}{\Sigma_{eq} + \frac{3\lambda+2\mu}{45\mu} A_1 \left({\Sigma_{eq}}^* - \Sigma_{eq}\right)} \left[{M_{mk}}^* - \frac{3\lambda+2\mu}{45\mu} \left({\Sigma_{eq}}^* - \Sigma_{eq}\right) U_k^p \right].$$

It follows from these expressions that

$$\begin{aligned} M_{ijk} &= M'_{ijk} + \delta_{ij} M_{mk} \\ &= \frac{\Sigma_{eq}}{\Sigma_{eq} + \frac{A_2}{5}\left({\Sigma_{eq}}^* - \Sigma_{eq}\right)} {M'_{ijk}}^* + \frac{\Sigma_{eq}}{\Sigma_{eq} + \frac{3\lambda+2\mu}{45\mu} A_1 \left({\Sigma_{eq}}^* - \Sigma_{eq}\right)} \delta_{ij} {M_{mk}}^* \\ &\quad - \frac{\Sigma_{eq}\left({\Sigma_{eq}}^* - \Sigma_{eq}\right)}{15\left[\Sigma_{eq} + \frac{A_2}{5}\left({\Sigma_{eq}}^* - \Sigma_{eq}\right)\right]} \left(\delta_{ik} U_j^p + \delta_{jk} U_i^p - \frac{2}{3} \delta_{ij} U_k^p \right) \\ &\quad - \frac{3\lambda+2\mu}{45\mu} \frac{\Sigma_{eq}\left({\Sigma_{eq}}^* - \Sigma_{eq}\right)}{\Sigma_{eq} + \frac{3\lambda+2\mu}{45\mu} A_1 \left({\Sigma_{eq}}^* - \Sigma_{eq}\right)} \delta_{ij} U_k^p \end{aligned}$$

so that

$$\begin{aligned} M_{ijj} = &\frac{\Sigma_{eq}}{\Sigma_{eq} + \frac{A_2}{5}\left({\Sigma_{eq}}^* - \Sigma_{eq}\right)} {M'_{ijj}}^* + \frac{\Sigma_{eq}}{\Sigma_{eq} + \frac{3\lambda+2\mu}{45\mu} A_1 \left({\Sigma_{eq}}^* - \Sigma_{eq}\right)} {M_{mi}}^* \\ &- \Sigma_{eq}\left({\Sigma_{eq}}^* - \Sigma_{eq}\right) \left[\frac{2}{9\left[\Sigma_{eq} + \frac{A_2}{5}\left({\Sigma_{eq}}^* - \Sigma_{eq}\right)\right]} + \frac{\frac{3\lambda+2\mu}{45\mu}}{\Sigma_{eq} + \frac{3\lambda+2\mu}{45\mu} A_1 \left({\Sigma_{eq}}^* - \Sigma_{eq}\right)} \right] U_i^p. \end{aligned}$$

Equation (1) then implies that

$$U_i^p = \frac{1}{{\Sigma_{eq}}^* - \Sigma_{eq}} \frac{\frac{{M'_{ijj}}^*}{\Sigma_{eq} + \frac{A_2}{5}\left({\Sigma_{eq}}^* - \Sigma_{eq}\right)} + \frac{{M_{mi}}^*}{\Sigma_{eq} + \frac{3\lambda+2\mu}{45\mu} A_1 \left({\Sigma_{eq}}^* - \Sigma_{eq}\right)}}{\frac{2}{9\left[\Sigma_{eq} + \frac{A_2}{5}\left({\Sigma_{eq}}^* - \Sigma_{eq}\right)\right]} + \frac{\frac{3\lambda+2\mu}{45\mu}}{\Sigma_{eq} + \frac{3\lambda+2\mu}{45\mu} A_1 \left({\Sigma_{eq}}^* - \Sigma_{eq}\right)}}, \qquad (32)$$

which is the relation looked for.

It follows from equation (32) that the vector $\mathbf{U}^p$ depends on the sole unknown Σ_{eq}. By equations (29) and (25), the same is true of the vector ${\mathbf{M}_m}^{**}$ and the tensor $\mathbf{M}'^{**}$, and also consequently of their invariants ${\mathcal{M}_1}^{**}$ and ${\mathcal{M}_2}^{**}$.

Using now the expressions (31), (27) of the invariants $\mathcal{M}_1$ and $\mathcal{M}_2$ and the definition (10) of the quadratic form Q^2, one gets

$$Q^2 = \Sigma_{eq}^2 \left\{ \frac{A_1 {\mathcal{M}_1}^{**}}{\left[\Sigma_{eq} + \frac{3\lambda+2\mu}{45\mu} A_1 \left({\Sigma_{eq}}^* - \Sigma_{eq}\right)\right]^2} + \frac{A_2 {\mathcal{M}_2}^{**}}{\left[\Sigma_{eq} + \frac{A_2}{5}\left({\Sigma_{eq}}^* - \Sigma_{eq}\right)\right]^2} \right\}.$$

Combination with equation $(18)_1$ then yields

$$\boxed{\Sigma_{eq}^2 \left\{ 1 + \frac{A_1 {\mathcal{M}_1}^{**}}{b^2 \left[\Sigma_{eq} + \frac{3\lambda+2\mu}{45\mu} A_1 \left({\Sigma_{eq}}^* - \Sigma_{eq} \right) \right]^2} + \frac{A_2 {\mathcal{M}_2}^{**}}{b^2 \left[\Sigma_{eq} + \frac{A_2}{5} \left({\Sigma_{eq}}^* - \Sigma_{eq} \right) \right]^2} \right\} = (1-p)^2 \Sigma^2 \cos^2 \phi.} \tag{33}$$

This is the second equation of the system looked for on the unknowns ϕ and Σ_{eq}. The left-hand side depends only on Σ_{eq} and the right-hand side only on ϕ.

The system of equations (23, 33) on ϕ and Σ_{eq} may be solved in different ways. Probably the simplest method consists of using equation (23) to express Σ_{eq} as a function of ϕ, and inserting its expression into equation (33) so as to get an equation on the single unknown ϕ, to be solved by Newton's method. But numerical experience that the convergence of the Newton iterations is then often problematic. An apparently less straightforward, but in reality more computationally efficient method is adopted here; this method consists of solving equation (23) on ϕ through Newton iterations, Σ_{eq} being calculated as a function of ϕ at each step by solving equation (33) through Newton sub-iterations.

Once ϕ and Σ_{eq} are known, the other unknowns Σ_m, $\mathbf{\Sigma}'$, $\mathbf{U}^p$, $\mathbf{M}'^{**}$, ${\mathbf{M}_m}^{**}$, $\mathbf{M}'$, $\mathbf{M}_m$ follow from equations $(18)_2$, (21), (32), (25), (29), (24) and (28).

3.4 Iterations on the hardening parameter

The value of the current yield stress Σ has been assumed to be known up to now. In reality it is not and must be determined iteratively. This is done using a fixed point algorithm [5], starting from the value at time t, solving the projection problem with this value, updating it using a discretized form of the evolution equation (16), re-solving the projection problem with the new value, etc. up to convergence.

In the discretized form of equation (16), $\mathbf{\Sigma} : \mathbf{D}^p + \mathbf{M} \vdots (\nabla \mathbf{D})^p$ is replaced by

$$\mathbf{\Sigma} : (\Delta \mathbf{E})^p + \mathbf{M} \vdots (\nabla \Delta \mathbf{E})^p = \Sigma'_{ij} {(\Delta E)_{ij}^p}' + 3\Sigma_m (\Delta E)_m^p + M'_{ijk} {(\nabla \Delta E)_{ijk}^p}' + 3 M_{mk} (\nabla \Delta E)_{mk}^p$$

where ${(\Delta E)_{ij}^p}'$, $(\Delta E)_m^p$, ${(\nabla \Delta E)_{ijk}^p}'$ and $(\nabla \Delta E)_{mk}^p$ are expressed using equations (20). This leads to the following expression of the increment of the hardening parameter E:

$$\Delta E = \frac{1}{(1-f)\Sigma} \left[\frac{\Sigma'_{ij} ({\Sigma'_{ij}}^* - \Sigma'_{ij})}{2\mu} + \frac{3\Sigma_m ({\Sigma_m}^* - \Sigma_m)}{3\lambda + 2\mu} + \frac{M'_{ijk} ({M'_{ijk}}^* - M'_{ijk})}{2\mu b^2/5} + \frac{3 M_{mk} ({M_{mk}}^* - M_{mk})}{(3\lambda + 2\mu) b^2/5} \right]. \tag{34}$$

[5] Such a rustic algorithm is sufficient because the variations of the yield stress are always quite small between successive instants.

3.5 Other features of the numerical implementation

The numerical implementation of the GLPD model, just like that of all second-gradient models, raises a difficulty tied to the apparent necessary use of the second derivatives of the shape functions. This seems to require elements of class $\mathcal{C}^1$ which, as a rule, are never available in standard FE codes. This difficulty is circumvented through some trick suggested by Gologanu *et al.* (1997) themselves and used since in a number of works (see for instance Shu *et al.* (1999), Forest *et al.* (2000), Matsushima *et al.* (2000)) for the numerical implementation of various second-gradient models. This trick consists of introducing a new nodal variable in the form of a symmetric second-rank tensor $\mathbf{W}$, replacing the gradient of the strain rate $\mathbf{D}$ by the gradient of $\mathbf{W}$ in all equations, and imposing the approximate coincidence of $\mathbf{W}$ and $\mathbf{D}$ at the Gauss points through some penalty method. The advantage is that the components of $\nabla\mathbf{D}$ are then obtained (in an approximate way) from the nodal values of the new variable $\mathbf{W}$ and the sole first derivatives of the shape functions; thus classical elements of class $\mathcal{C}^0$ are sufficient. Of course, the price to pay is an increased number of nodal degrees of freedom: six $(V_1, V_2, W_{11}, W_{22}, W_{12}, W_{33})$ instead of two (V_1, V_2) in 2D.

Imposing the internal constraints $W_{ij} - D_{ij} = 0$ by a penalty method may of course give rise to locking phenomena, for which subintegration is the natural remedy. In practice, 8-node quadratic elements are used with 4-Gauss points integration. Numerical experience reveals that this is sufficient to prevent locking.

Finally, in the axisymmetric case, one needs the expression of the gradient of the tensorial variable $\mathbf{W}$ in cylindrical coordinates R, Θ, Z. Standard calculation techniques lead to the following expressions of the components of this gradient (in the sole case of interest where $\mathbf{W}$ is independent of Θ and the components $W_{R\Theta}$ and $W_{Z\Theta}$ nil):

$$\left\{\begin{array}{l}(\nabla W)_{RRR} = W_{RR,R}\\ (\nabla W)_{\Theta\Theta R} = W_{\Theta\Theta,R}\\ (\nabla W)_{RZR} = W_{RZ,R}\\ (\nabla W)_{ZZR} = W_{ZZ,R}\end{array}\right. , \quad \left\{\begin{array}{l}(\nabla W)_{R\Theta\Theta} = \dfrac{W_{RR} - W_{\Theta\Theta}}{R}\\ (\nabla W)_{Z\Theta\Theta} = \dfrac{W_{RZ}}{R}\end{array}\right. , \quad \left\{\begin{array}{l}(\nabla W)_{RRZ} = W_{RR,Z}\\ (\nabla W)_{\Theta\Theta Z} = W_{\Theta\Theta,Z}\\ (\nabla W)_{RZZ} = W_{RZ,Z}\\ (\nabla W)_{ZZZ} = W_{ZZ,Z}.\end{array}\right. \tag{35}$$

4 Analytic solution for the circular bending of a beam in plane strain - Assessment of the programme

In order to provide a reference solution for the assessment of the programme, we shall now derive an analytic solution of the problem of the circular bending of a beam in plane strain, in the limiting case of a zero porosity.

4.1 Generalities

Figure 1 depicts the problem to be solved. A beam of rectangular cross-section, center O, thickness $2h$, parallel to the direction OX, obeying the equations of the GLPD model, is bent in plane strain in the plane OXY. The lateral boundary conditions enforce a linear variation of the horizontal strain component E_{XX} upon the vertical coordinate Y.

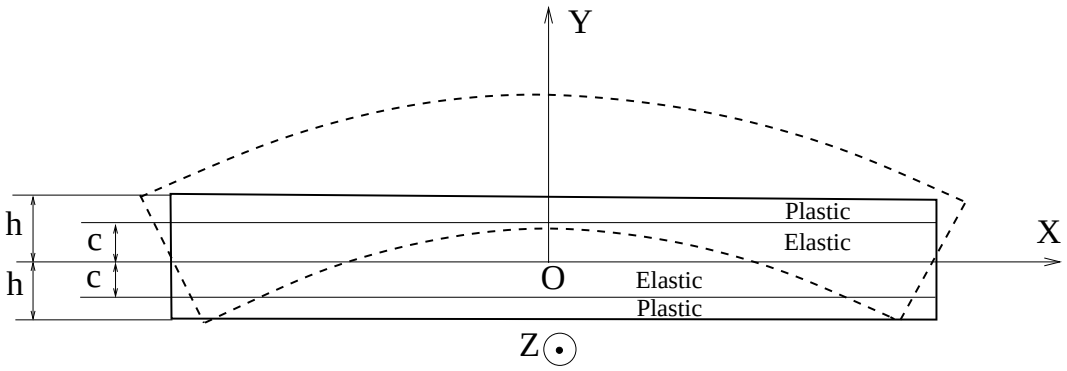

Fig. 1. Circular bending of a beam in plane strain

In order for an analytic solution to be workable, it reveals necessary to make the assumption of a zero porosity. This makes the solution somewhat academic, since the only reason for developing the GLPD model was to avoid unrealistic localization of strain and damage *arising from the presence of some porosity!* In spite of this, the solution developed will be interesting for two reasons:

- For the assessment of the programme, the important point is not that the reference solution be of major practical significance, but that it be analytic and explicit.
- In the case of a zero porosity, the stress and moment tensors $\mathbf{\Sigma}(\mathbf{X})$, $\mathbf{M}(\mathbf{X})$ of the GLPD model should represent the average values, over the sphere of center $\mathbf{X}$ and radius b, of the zeroth- and first-order moments of the stress tensor $\boldsymbol{\sigma}(\mathbf{x})$ of a sound (void-free) von Mises material. (See Appendix A on the micromechanical foundations of the GLPD model). Checking such a coincidence, at least approximately, in the specific case considered will allow to assess the physical soundness of the GLPD model itself.

The problem will be solved within the linearized context: small displacements, small strains. Various hypotheses will be made successively on the material behavior: purely elastic, purely plastic and finally elastic-plastic.

In all cases the strain field found will be of the form

$$\begin{cases} E_{XX} & = CY \\ E_{YY} & = g(Y) \\ \text{other } E_{ij} & = 0, \end{cases} \tag{36}$$

C being a constant (representing the curvature of the neutral fiber $Y = 0$) and $g(Y)$ a given function. Such a strain field obeys the compatibility conditions and thus derives from some displacement field, the precise form of which will not be provided.

The equilibrium equations and the boundary conditions on the upper and lower surfaces will obviously be needed. These equations are easily deduced from the principle of virtual work, combined with the expressions (2), (3) of the virtual powers of internal and external forces, and read [6]:

$$\begin{cases} \Sigma_{ij,j} - M_{ijk,jk} = 0 & \text{in } \Omega \\ \Sigma_{XY} = \Sigma_{YY} = \Sigma_{ZY} = 0 & \text{for } Y = \pm h \\ M_{XYY} = M_{YYY} = M_{ZYY} = 0 & \text{for } Y = \pm h. \end{cases} \tag{37}$$

4.2 Purely elastic solution

In the case of a purely elastic behavior, the relations between the stress and moment tensors and the strain tensor and its gradient are given by equations (5) and (7), with Σ_{ij}, M_{ijk}, E_{ij} and $E_{ij,k}$ instead of $D\Sigma_{ij}/Dt$, DM_{ijk}/Dt, D^e_{ij} and $(\nabla D)^e_{ijk}$.

Let us first determine the strain and stress fields. We are looking for a solution in which all stress components are zero except Σ_{XX} and Σ_{ZZ}. The condition of plane strain then yields, by equation $(5)_1$:

$$E_{ZZ} = \frac{\Sigma_{ZZ}}{E} - \frac{\nu\Sigma_{XX}}{E} = 0 \quad \Rightarrow \quad \Sigma_{ZZ} = \nu\Sigma_{XX}$$

where E and ν denote Young's modulus and Poisson's ratio. It follows, again by equation $(5)_1$, that

$$E_{XX} = CY = \frac{\Sigma_{XX}}{E} - \frac{\nu\Sigma_{ZZ}}{E} = \frac{1-\nu^2}{E}\,\Sigma_{XX} \quad \Rightarrow \quad \Sigma_{XX} = \frac{E}{1-\nu^2}\,CY.$$

Therefore the stress field is given by

$$\begin{cases} \Sigma_{XX} = \dfrac{E}{1-\nu^2}\,CY \\ \Sigma_{ZZ} = \dfrac{E\nu}{1-\nu^2}\,CY \\ \text{other } \Sigma_{ij} = 0, \end{cases} \tag{38}$$

and the strain field immediately follows from there:

$$\begin{cases} E_{XX} = CY \\ E_{YY} = -\dfrac{\nu}{1-\nu}\,CY \\ \text{other } E_{ij} = 0. \end{cases} \tag{39}$$

[6] Discarding terms of the form $M_{iXY,X}$ and $M_{iZY,Z}$ in equation $(37)_2$ since the stress and moment fields are obviously independent of X and Z.

Let us now determine the strain gradient and the moment tensor. The components of the strain gradient follow from those of the strain:

$$\begin{cases} E_{XX,Y} & = C \\ E_{YY,Y} & = -\dfrac{\nu}{1-\nu} C \\ \text{other } E_{ij,k} & = 0. \end{cases} \tag{40}$$

The vector $\mathbf{U}^e$ defined by equation (7) is then easily checked to be zero, and equation $(5)_2$ yields the components of the moment tensor:

$$\begin{cases} M_{XXY} & = \dfrac{E}{1-\nu^2}\dfrac{b^2}{5} C \\ M_{ZZY} & = \dfrac{E\nu}{1-\nu^2}\dfrac{b^2}{5} C \\ \text{other } M_{ijk} & = 0. \end{cases} \tag{41}$$

It is easy to see that the stress and moment fields thus determined do verify the equilibrium equations and boundary conditions (37). Thus the purely elastic solution is complete.

4.3 Purely plastic solution

We shall now look for a solution for a purely plastic behavior, assuming the curvature C of the neutral fiber to be an increasing function of time ($\dot{C} > 0$). For such a material behavior, the elastic parts of the strain rate and its gradient are zero and their plastic parts are given by the flow rule (12). It will also be assumed that the material is ideal-plastic so that the "average yield stress" Σ is identical to that of the virgin material, σ_0, and that the porosity is zero.

We shall look for a solution in which the beam is entirely plastic, so that the yield function $\Phi(\mathbf{\Sigma}, \mathbf{M})$ is zero everywhere. No such solution exists for a von Mises material, for which the vanishing of all stress components on the neutral fiber implies the necessary existence of some elastic (or rigid) core around this fiber. For a material obeying the GLPD model, however, such a solution can be found because the yield function (8) involves the components of the moment tensor, which do not vanish on the neutral fiber.

Consider the strain rate and stress fields first. The purely elastic solution suggests that all strain rate components should be zero except D_{XX} and D_{YY}. Furthermore the flow rule $(12)_1$, where the derivatives $\partial\Phi/\partial\Sigma_{ij}$ are given by equation $(13)_1$ with $p = 0$, implies that the material is incompressible ($\operatorname{tr}\mathbf{D} = 0$). Therefore the strain rate field is given by

$$\begin{cases} D_{XX} & = \dot{C}Y \\ D_{YY} & = -\dot{C}Y \\ \text{other } D_{ij} & = 0. \end{cases} \tag{42}$$

The purely elastic solution also suggests that all stress components should be zero except Σ_{XX} and Σ_{ZZ}. The flow rule $(12)_1$ then reduces to

$$\begin{cases} D_{XX} = \dot{C}Y & = \dfrac{3H}{\sigma_0^2}\left(\Sigma_{XX} - \Sigma_m\right) \\ D_{YY} = -\dot{C}Y & = -\dfrac{3H}{\sigma_0^2}\Sigma_m \\ D_{ZZ} = 0 & = \dfrac{3H}{\sigma_0^2}\left(\Sigma_{ZZ} - \Sigma_m\right) \end{cases}$$

where $\Sigma_m = \frac{1}{3}(\Sigma_{XX} + \Sigma_{ZZ})$, so that the nonzero stress components are given in terms of the plastic multiplier H by

$$\begin{cases} \Sigma_{XX} = \dfrac{2\sigma_0^2}{3H}\,\dot{C}Y \\ \Sigma_{ZZ} = \dfrac{\sigma_0^2}{3H}\,\dot{C}Y. \end{cases} \tag{43}$$

Consider now the gradient of the strain rate and the moment tensor. The former tensor is given by

$$\begin{cases} D_{XX,Y} & = \dot{C} \\ D_{YY,Y} & = -\dot{C} \\ \text{other } D_{ij,k} & = 0. \end{cases} \tag{44}$$

The purely elastic solution suggests that all moment components should be zero except M_{XXY} and M_{ZZY}. Then the flow rule $(12)_2$ (where the derivatives $\partial\Phi/\partial M_{ijk}$ are given by equation $(13)_2$) reduces to the following equations:

- For $k = X$:

$$U_X^p = U_Y^p = 0. \tag{45}$$

- For $k = Y$ (account being taken of equation (45)):

$$\begin{cases} D_{XX,Y} = \dot{C} & = \dfrac{H}{\sigma_0^2 b^2}\left[\left(\dfrac{2A_1}{3} - 3A_2\right)M_{mY} + 3A_2 M_{XXY}\right] \\ D_{YY,Y} = -\dot{C} & = \dfrac{H}{\sigma_0^2 b^2}\left(\dfrac{2A_1}{3} - 3A_2\right)M_{mY} \\ D_{ZZ,Y} = 0 & = \dfrac{H}{\sigma_0^2 b^2}\left[\left(\dfrac{2A_1}{3} - 3A_2\right)M_{mY} + 3A_2 M_{ZZY}\right] \end{cases} \tag{46}$$

  where $M_{mY} = \frac{1}{3}(M_{XXY} + M_{ZZY})$.

Taking the sum of equations (46), one gets

$$3\left(\frac{2A_1}{3} - 3A_2\right)M_{mY} + 3A_2(M_{XXY} + M_{ZZY}) = 0 \quad \Rightarrow \quad \frac{2A_1}{3}(M_{XXY} + M_{ZZY}) = 0,$$

which is possible only if

$$A_1 = 0. \tag{47}$$

In other words, if the constant A_1 is nonzero, the solution cannot be of the type looked for here, with all moment components nil except M_{XXY} and M_{ZZY}. Unfortunately the value

of A_1 provided by equation $(10)_2$ *is* nonzero! It is therefore necessary to momentarily modify it and set it to zero, for the sake of comparison between the analytic solution developed and the numerical results. Such a modification is harmless because (i) the primary concern here is not physical realism but validation of the programme and (ii) the resulting change of the model is quite minor anyway, the true value of A_1 being much smaller than that of A_2 (see equations $(10)_2$ and $(10)_3$).

Making hypothesis (47) and solving equations (46) with respect to the moment components, one gets

$$\begin{cases} M_{XXY} = \dfrac{2\sigma_0^2 b^2}{3HA_2}\,\dot{C} \\ M_{ZZY} = \dfrac{\sigma_0^2 b^2}{3HA_2}\,\dot{C}. \end{cases} \tag{48}$$

To complete the determination of the stress and moment fields, let us calculate the plastic multiplier H by combining the yield criterion (8) with equations (43) and (48); the result is

$$H = \frac{\sigma_0}{\sqrt{3}}\,\dot{C}\,\sqrt{Y^2 + \frac{b^2}{A_2}}. \tag{49}$$

The stress and moment fields follow:

$$\begin{cases} \Sigma_{XX} = \dfrac{2\sigma_0}{\sqrt{3}}\,\dfrac{Y}{\sqrt{Y^2 + b^2/A_2}} \\ \Sigma_{ZZ} = \dfrac{\sigma_0}{\sqrt{3}}\,\dfrac{Y}{\sqrt{Y^2 + b^2/A_2}} \\ \text{other } \Sigma_{ij} = 0 \end{cases} \quad ; \quad \begin{cases} M_{XXY} = \dfrac{2\sigma_0}{\sqrt{3}A_2}\,\dfrac{b^2}{\sqrt{Y^2 + b^2/A_2}} \\ M_{ZZY} = \dfrac{\sigma_0}{\sqrt{3}A_2}\,\dfrac{b^2}{\sqrt{Y^2 + b^2/A_2}} \\ \text{other } M_{ijk} = 0. \end{cases} \tag{50}$$

The stress and moment fields thus determined obviously verify the equilibrium equations and boundary conditions (37). Thus the purely plastic solution is complete.

4.4 Elastic-plastic solution

We shall now look for an elastic-plastic solution involving an elastic zone $-c \leq Y \leq c$ and two plastic zones $Y < -c$ and $Y > c$, c being a parameter to be determined as a function of the load parameter C (see Figure 1).

This solution will be required to coincide with the purely elastic solution determined in Subsection 4.2 in the elastic zone, and with the purely plastic solution determined in Subsection 4.3 in the plastic zones. For the latter solution, which disregards elasticity, to be applicable in the plastic zones, it is necessary that the elastic parts of the strain rate and its gradient, and consequently the rates of the stress and moment tensors, be zero in these zones. These conditions are compatible with the expressions (50) of the stress and moment tensors which are independent of C and $\dot{C}$ and therefore constant in time.

Thus in the solution looked for, the position of the boundaries $Y = -c$, $Y = c$ of the

plastic zones will vary in time, but the spatial distributions of the stress and moment tensors within these zones will not. On the other hand, in the elastic zone $\mathbf{\Sigma}$ will vary linearly with Y between the values $\mathbf{\Sigma}(-c)$ and $\mathbf{\Sigma}(c)$, $\mathbf{M}$ will be uniform, and both will depend on time. These features are identical to those of the solution for a von Mises material. However the distribution of the stresses in the plastic zones will be found to be non-uniform, in contrast to what happens for a von Mises material.

Some conditions must be fulfilled for the elastic-plastic solution to be of the type looked for here:

- Condition (47) is necessary for the purely plastic solution studied in Subsection 4.3 to be applicable.
- In the elastic zone, $\Sigma_{ZZ} = \nu\Sigma_{XX}$ and $M_{ZZY} = \nu M_{XXY}$ (see equations (38) and (41)), whereas in the plastic zones, $\Sigma_{ZZ} = \frac{1}{2}\Sigma_{XX}$ and $M_{ZZY} = \frac{1}{2}M_{XXY}$ (see equations (50)). Therefore for the stresses and moments to be continuous on the interfaces between the elastic and plastic zones, it is necessary that

$$\nu = \frac{1}{2}. \tag{51}$$

  The material is then incompressible so that the strain rate and its gradient are given by equations (42) and (44) in the whole structure.
- The additional condition (56) will reveal below to be necessary.

Consider first the stress and moment fields in the elastic zone $-c \leq Y \leq c$. These fields are given by equations (38) and (41) with the condition (51):

$$\left\{\begin{array}{ll} \Sigma_{XX} & = \dfrac{4E}{3}\,CY \\ \Sigma_{ZZ} & = \dfrac{2E}{3}\,CY \\ \text{other } \Sigma_{ij} & = 0, \end{array}\right. \quad ; \quad \left\{\begin{array}{ll} M_{XXY} & = \dfrac{4Eb^2}{15}\,C \\ M_{ZZY} & = \dfrac{2Eb^2}{15}\,C \\ \text{other } M_{ijk} & = 0. \end{array}\right. \tag{52}$$

These equations allow for the calculation of the half-thickness c of the elastic zone. Indeed, writing the criterion (8) on the boundary of the elastic zone, at $Y = \pm c$, one gets

$$\frac{4E^2}{3}C^2\left(c^2 + \frac{A_2}{25}b^2\right) = \sigma_0^2 \quad \Rightarrow \quad c = \sqrt{\frac{3\sigma_0^2}{4E^2C^2} - \frac{A_2}{25}b^2}\,. \tag{53}$$

Two values of the load parameter C are of special interest, that for which c is equal to the half-thickness h of the beam, C_h, and that for which c is zero, C_0:

$$\left\{\begin{array}{l} C_h \equiv \dfrac{\sigma_0}{2E}\sqrt{\dfrac{3}{h^2 + \frac{A_2}{25}b^2}} \\ C_0 \equiv \dfrac{5\sigma_0}{2Eb}\sqrt{\dfrac{3}{A_2}}\,. \end{array}\right. \tag{54}$$

These values mark transitions between solutions of different types:

- If $C < C_h$, the beam is entirely elastic: $c = h$. (Equation $(53)_2$ does not apply because the yield limit is not reached even at $Y = \pm h$).
- If $C_h \leq C \leq C_0$, the beam is partially elastic, partially plastic; the value of c is provided by equation $(53)_2$ and lies between 0 and h.
- If $C > C_0$, the beam is entirely plastic: $c = 0$, and the limit-load is reached. (Equation $(53)_2$ does not apply because there is no elastic zone).

Consider now the stress and moment fields in the plastic zones $Y < -c$ and $Y > c$. These fields are given by equations (50). Therefore the continuity of the stress and moment components Σ_{XX}, M_{XXY} [7] at the interfaces between the elastic and plastic zones implies, by equations (52), that

$$\left\{\begin{array}{ll} \dfrac{4E}{3}\,Cc &= \dfrac{2\sigma_0}{\sqrt{3}}\,\dfrac{c}{\sqrt{c^2+b^2/A_2}} \\ \dfrac{4Eb^2}{15}\,C &= \dfrac{2\sigma_0}{\sqrt{3}A_2}\,\dfrac{b^2}{\sqrt{c^2+b^2/A_2}} \end{array}\right. \quad \Rightarrow \quad \left\{\begin{array}{l} \dfrac{2E}{\sqrt{3}}\,C = \dfrac{\sigma_0}{\sqrt{c^2+b^2/A_2}} \\ \dfrac{2E}{\sqrt{3}}\,C = \dfrac{5\sigma_0/A_2}{\sqrt{c^2+b^2/A_2}}, \end{array}\right. \tag{55}$$

which is possible only if

$$A_2 = 5. \tag{56}$$

Again, we shall momentarily adopt this new value of A_2 for the sake of comparison between the analytic solution developed and the numerical results. Note that the modified value is close to the true one provided by equation $(10)_3$ anyway. With this value of A_2, the continuity conditions (55) reduce to equation $(53)_1$ and are thus automatically satisfied.

With condition (56), equations $(53)_2$ and (54) for c, C_h and C_0 become

$$c = \sqrt{\frac{3\sigma_0^2}{4E^2C^2} - \frac{b^2}{5}} \quad ; \quad \left\{\begin{array}{l} C_h \equiv \dfrac{\sigma_0}{2E}\sqrt{\dfrac{3}{h^2+b^2/5}} \\ C_0 \equiv \dfrac{\sqrt{15}}{2}\,\dfrac{\sigma_0}{Eb}, \end{array}\right. \tag{57}$$

and the expressions of the stress and moment fields in the plastic zones become

$$\left\{\begin{array}{ll} \Sigma_{XX} & = \dfrac{2\sigma_0}{\sqrt{3}}\,\dfrac{Y}{\sqrt{Y^2+b^2/5}} \\ \Sigma_{ZZ} & = \dfrac{\sigma_0}{\sqrt{3}}\,\dfrac{Y}{\sqrt{Y^2+b^2/5}} \\ \text{other } \Sigma_{ij} & = 0 \end{array}\right. \quad ; \quad \left\{\begin{array}{ll} M_{XXY} & = \dfrac{2\sigma_0}{5\sqrt{3}}\,\dfrac{b^2}{\sqrt{Y^2+b^2/5}} \\ M_{ZZY} & = \dfrac{\sigma_0}{5\sqrt{3}}\,\dfrac{b^2}{\sqrt{Y^2+b^2/5}} \\ \text{other } M_{ijk} & = 0. \end{array}\right. \tag{58}$$

The stress and moment fields defined by equations (52) and (58) satisfy the equilibrium equations [8] and the boundary conditions (37), so that the elastic-plastic solution is complete.

[7] There is no need to write the additional continuity of Σ_{ZZ} and M_{ZZY} since $\Sigma_{ZZ} = \frac{1}{2}\Sigma_{XX}$ and $M_{ZZY} = \frac{1}{2}M_{XXY}$ everywhere.

[8] Including the necessary requirements of continuity at the interfaces between the elastic and plastic zones.

4.5 Comparison with numerical results and comments

The mesh used in the numerical calculations is composed of 20 square quadratic subintegrated elements (8 nodes and 4 Gauss points per element). There are 2 elements in the direction X and 10 elements in the direction Y. The thickness of the beam is $2h = 10$ mm. The values of Young's modulus E, Poisson's ratio ν, the yield limit σ_0 and the microstructural distance b are 203,000 MPa, 0.5, 450 MPa and 1 mm respectively. The porosity is zero and the constants A_1 and A_2 are given by equations (47) and (56).

Comparisons have been performed for the three types of solutions studied: purely elastic, purely plastic and elastic-plastic, but results will be shown for the sole elastic-plastic solution for space reasons. Figures 2 and 3 compare the analytical and numerical distributions of the stress component Σ_{XX} and the moment component M_{XXY} at a typical stage of the loading. In these figures the discrete points represent the numerical results, the dotted straight lines the theoretical purely elastic solution and the hatched curved lines the theoretical purely plastic solution. One can see that the numerical results agree very well with the "composite" elastic-plastic solution which consists of the purely elastic solution in the central elastic zone and the purely plastic solution in the outer plastic zones.

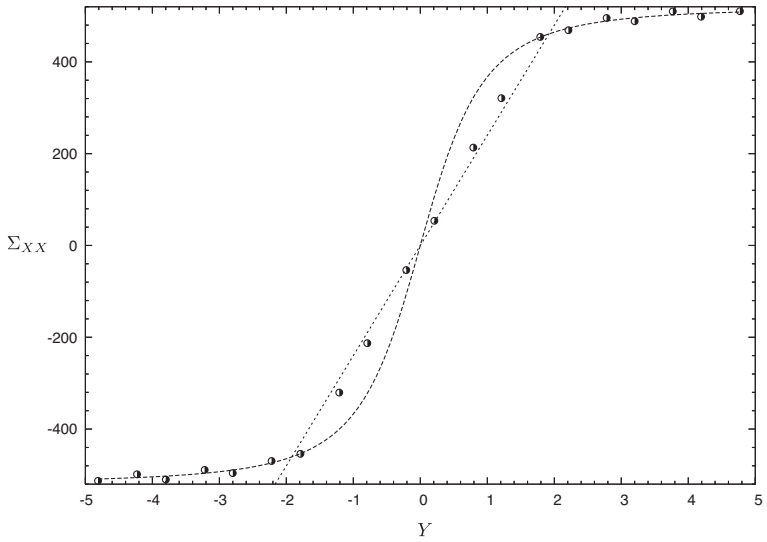

Fig. 2. Comparison of analytical and numerical values of Σ_{XX} - Y in mm, Σ_{XX} in MPa

Another more basic comment is in order here. Let $\sigma_{XX}(y)$ denote the stress which would be obtained for a von Mises material. In the elastic zone σ_{XX} is identical to the stress Σ_{XX} for a GLPD material, but in the plastic zones it is uniform, equal to $-2\sigma_0/\sqrt{3}$ for $y < -c$ and $2\sigma_0/\sqrt{3}$ for $y > c$. Also, let $\langle\sigma_{XX}\rangle(Y)$ represent the average value of $\sigma_{XX}(y)$ over the sphere of center Y and radius b. Clearly, outside of the small intervals $(-c-b, -c+b)$, $(c-b, c+b)$ centered at the elastic-plastic interfaces, the distribution of $\langle\sigma_{XX}\rangle$ is identical to that of σ_{XX}, that is linear in the elastic zone and uniform in the plastic zones; and in the "transition" intervals $(-c-b, -c+b)$, $(c-b, c+b)$ it is quadratic, the derivative $d\langle\sigma_{XX}\rangle/dy$ being continuous at the points $-c-b$, $-c+b$, $c-b$, $c+b$. This distribution closely resembles that of the stress Σ_{XX} for a GLPD material, the only significant difference being that in the plastic zones $\langle\sigma_{XX}\rangle$ becomes constant and equal to $\pm 2\sigma_0/\sqrt{3}$ as soon as $|Y|$ becomes larger than $c+b$, whereas Σ_{XX} reaches the

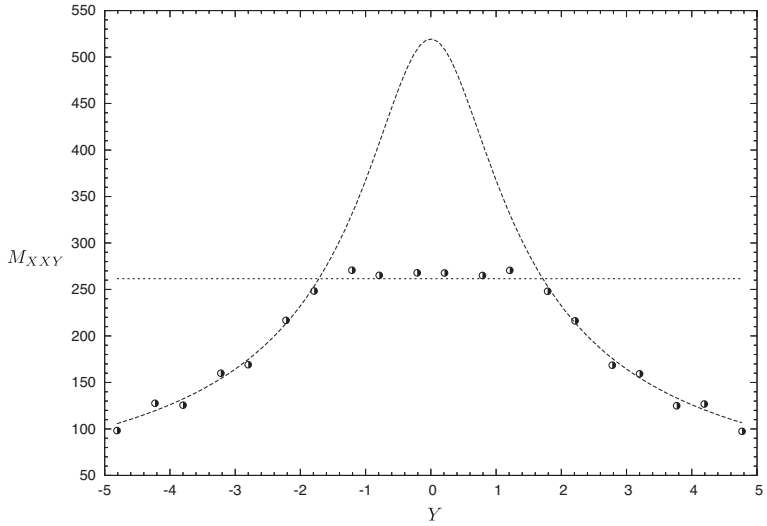

Fig. 3. Comparison of analytical and numerical values of M_{XXY} - Y in mm, M_{XXY} in MPa.m

value $\pm 2\sigma_0/\sqrt{3}$ only asymptotically, for large values of $|Y|$. Similarly, one easily sees that the distribution of the average value of $\sigma_{XX}(y)(y-Y)$ over the sphere of center Y and radius b is analogous to that of the moment M_{XXY}. Again, the only significant difference is that this average value is strictly zero for $|Y| > c + b$ whereas M_{XXY} goes to zero only asymptotically, for large values of $|Y|$.

The conclusion is that in the problem investigated, the distributions of the stress and moment tensors $\mathbf{\Sigma}(\mathbf{X})$, $\mathbf{M}(\mathbf{X})$ are analogous to those of the average values, over the sphere of center $\mathbf{X}$ and radius b, of the zeroth- and first-order moments of the stress tensor $\boldsymbol{\sigma}(\mathbf{x})$ of a sound von Mises material. These distributions are precisely what the micromechanical foundations of the GLPD model suggest they should be, in such a case of zero porosity. This illustrates the physical soundness of this model.

5 Numerical applications

5.1 Verification of absence of mesh size effects

The first task is to check that use of the GLPD model allows to eliminate mesh size effects observed in numerical computations based on Gurson's standard model. No comparison with experimental results is needed for this purpose. A simple imaginary pre-notched axisymmetric tensile specimen made of A508 Cl.3 steel (American standard) is therefore considered. A fine mesh of this specimen consisting of quadratic triangles and quadratic subintegrated quadrangles is shown in Figure 4; a cruder mesh with twice as big elements in the central region of the notch is also used. Advantage is taken of symmetry about the horizontal mid-plane to mesh only the upper half of the structure. The semi-height and radius are 5 mm and 4 mm respectively. The shape of the central notch is rectangular in a meridian plane, with semi-width 0.3 mm and depth 1 mm. The values of the material parameters are $E = 203,000$ MPa, $\nu = 0.3$, σ_0 (initial yield stress) = 450 MPa, $q = 1.47$, f_0 (initial porosity) = 0.00016, $f_c = 0.0005$ and $\delta = 2.8$.

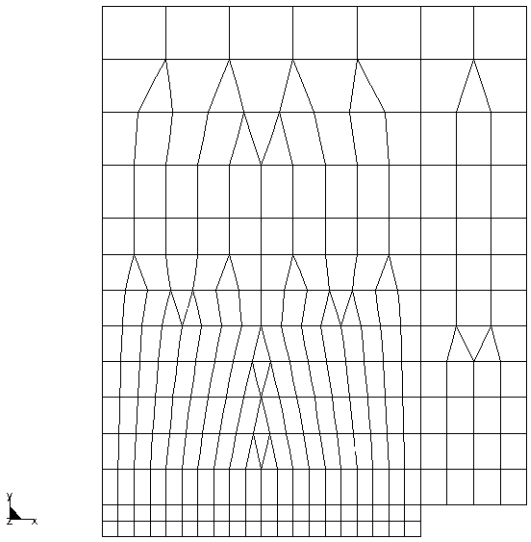

Fig. 4. Fine mesh of a pre-notched specimen

Figure 5 shows the load-displacement curve obtained with both meshes, using the standard Gurson model. The numbers in the upper right corner refer to the size of the square elements used in the region ahead of the notch root. There is a notable effect of mesh size in the softening region of the curves.

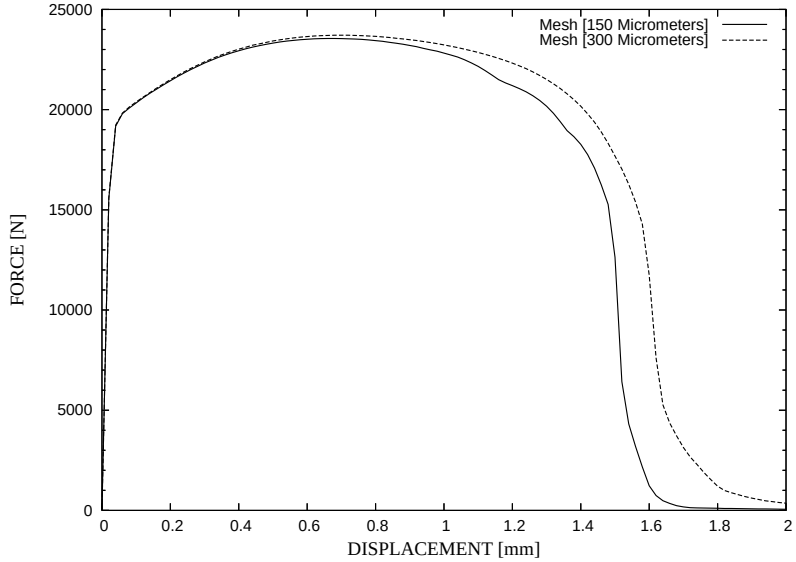

Fig. 5. Effect of mesh size upon the load-displacement curve of a pre-notched specimen - Gurson model

Figure 6 shows the results obtained with the GLPD model in a similar way. The value of the microstructural distance used is $b = 2$ mm [9] . The discrepancy between the two curves is greatly reduced, as desired, if not completely eliminated.

[9] This is admittedly a very large value for a "microstructural" length, but this is of little importance here since no experimental results are available for comparison.

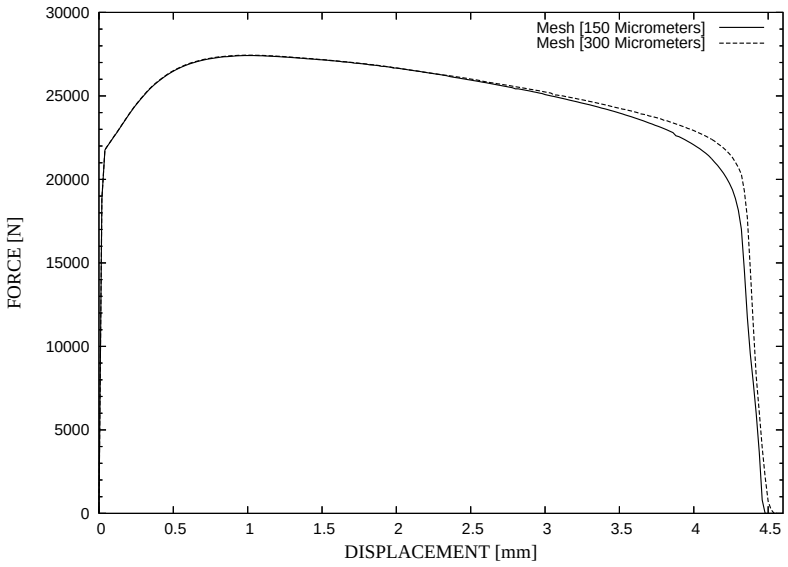

Fig. 6. Effect of mesh size upon the load-displacement curve of a pre-notched specimen - GLPD model

5.2 Numerical simulation of typical ductile fracture tests

Modifications of the standard Gurson model aimed at avoiding unlimited localization of strain and damage may well result in a significant degradation of the agreement between numerical predictions and results of typical ductile fracture tests. This was for instance the case with Leblond *et al.* (1994)'s first version of a nonlocal evolution equation for the porosity, prior to the modification introduced by Enakoutsa *et al.* (2007). The question of agreement of the model predictions with experiments is thus not only essential, but definitely non-trivial.

To investigate this question, we shall consider three homothetical pre-cracked axisymmetric tensile specimens (TA15, TA30, TA50, where the number refers to the diameter), again made of A508 Cl.3 steel, for which experimental results of fracture tests have been provided by Rousselier and Mudry (1980). The three meshes are shown in Figure 7. (The impression that the three geometries are identical is erroneous and due to the use of different magnification factors; the minimum element size, 0.2 mm, is in fact the same in all cases). Again, advantage is taken of symmetry about the horizontal mid-plane to mesh only the upper half of the specimens. Their semi-height and radius are as follows: TA15, 22.5 mm and 7.5 mm; TA30, 45 mm and 15 mm; TA50, 75 mm and 25 mm. The shape of the central notch is triangular in a meridian plane; its half-opening angle is 30° and its depth is 2.5 mm (TA15), 5 mm (TA30) or 8.3 mm (TA50). A fatigue pre-crack (invisible in the figure) of length 0.9 mm (TA15), 1.7 mm (TA30) or 2.85 mm (TA50) originates from the notch root. The material parameters are the same as in Subsection 5.1, except that a more realistic value of 0.55 mm is used for the microstructural distance b.

Figures 8, 9 and 10 show the experimental load-displacement curves (in the form of discrete points) together with the numerical predictions (in the form of full lines) for the three specimens. The agreement is quite acceptable in all cases in view of the experimental errors.

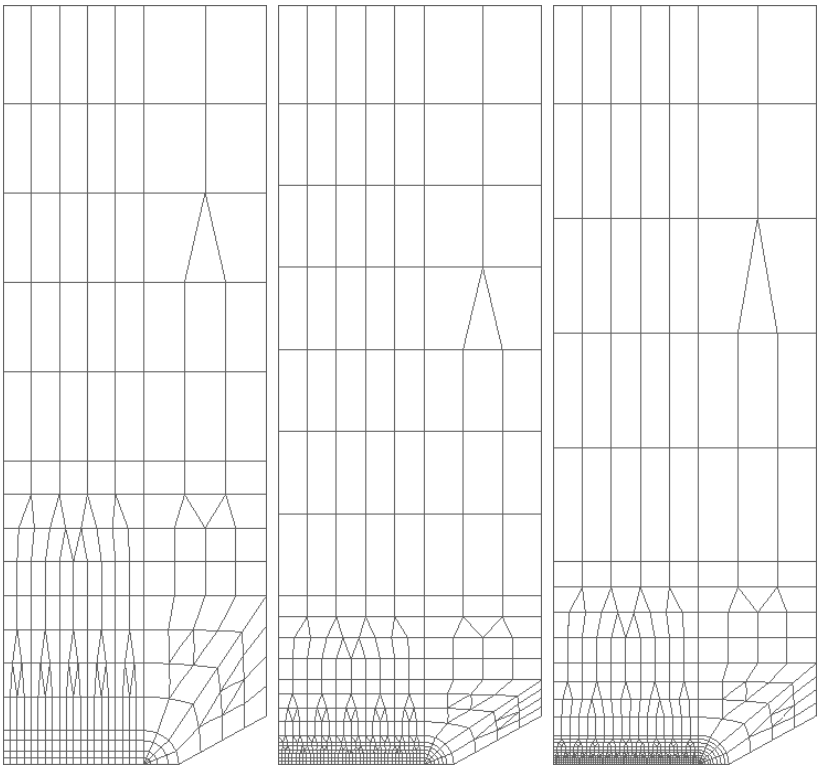

Fig. 7. Meshes of TA specimens. Left: TA15, center: TA30, right: TA50

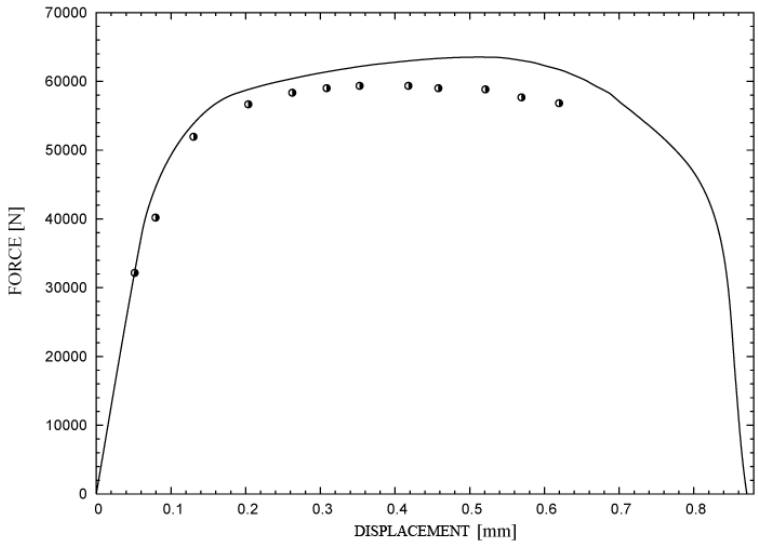

Fig. 8. Comparison of experimental and numerical load-displacement curves of a pre-cracked TA15 specimen

6 Conclusion

The GLPD micromorphic model of ductile rupture has been implemented into some FE programme. The major ingredient of the implementation consists of an implicit (backward Euler) algorithm used to solve the problem of projection of the elastic stress predictor onto the complex GLPD yield locus. This algorithm ensures existence and uniqueness of the solution. The problem is reduced to numerically solving a system of two equations on

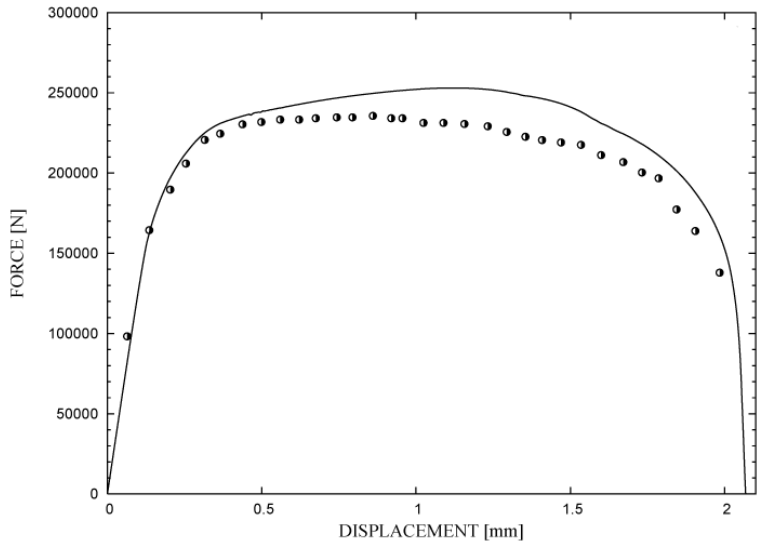

Fig. 9. Comparison of experimental and numerical load-displacement curves of a pre-cracked TA30 specimen

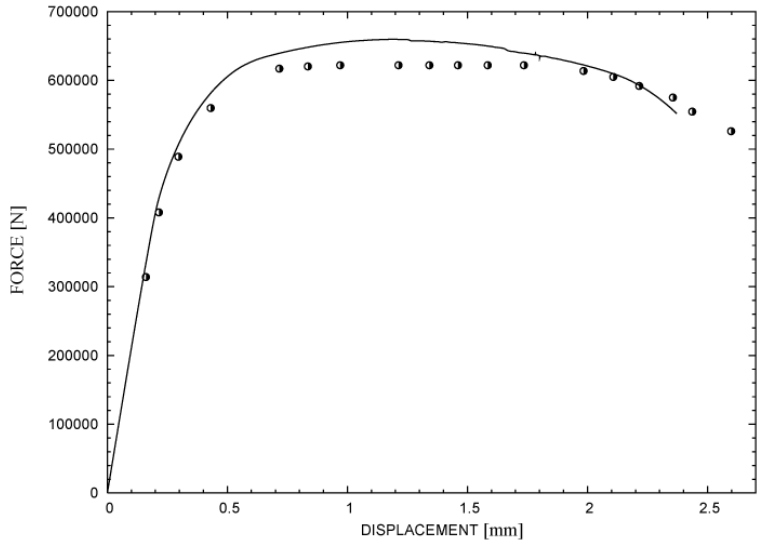

Fig. 10. Comparison of experimental and numerical load-displacement curves of a pre-cracked TA50 specimen

two scalar unknowns.

An analytic solution has then been found to the problem of plane strain circular bending of a beam obeying the equations of the GLPD model with a zero porosity. Interestingly, this solution can be used to assess not only the programme developed but also, to some extent, the basic physical soundness of the GLPD model. The conclusions of both of these assessments are positive.

Numerical applications have finally been presented with a double aim: (i) check that mesh size effects are no longer present in FE computations when the GLPD model is used instead of Gurson's; (ii) examine the quality of the agreement between numerical predictions and experimental results for some typical ductile rupture tests. The conclusion is that the GLPD model passes the two tests. It may thus be regarded as a viable solution

to the problem of unlimited localization of strain and damage in Gurson's model.

However numerical computations using the GLPD model are quite time-consuming, obviously because of the increased number of nodal degrees of freedom. Also, convergence of the global iterations aimed at simultaneously satisfying the equilibrium equations, the yield criterion and the plastic flow rule, often reveals difficult. These are good reasons not to reject cruder but simpler solutions to the problem of unlimited localization, like for instance Leblond *et al.* (1994)'s heuristic proposal, recently improved by Enakoutsa *et al.* (2007), of use of some nonlocal evolution equation for the porosity within an otherwise unmodified Gurson model.

References

Aravas N. (1987). On the numerical integration of a class of pressure-dependent plasticity models, *Int. J. Num. Meth. Engng.*, **24**, 1395-1416.

Enakoutsa K. (2007). Modèles non-locaux en rupture ductile des métaux, Ph.D. thesis, Université Pierre et Marie Curie (Paris VI) (in French).

Enakoutsa K., Leblond J.B. and Perrin G. (2007). Numerical implementation and assessment of a phenomenological nonlocal model of ductile rupture, *Comput. Meth. Appl. Mech. Engng.*, **196**, 1946-1957.

Forest S., Barbe F. and Cailletaud G. (2000). Cosserat modelling of size effects in the mechanical behaviour of polycrystals and multi-phase materials, *Int. J. Solids Structures*, **37**, 7105-7126.

Gologanu M., Leblond J.B., Perrin G. and Devaux J. (1997). Recent extensions of Gurson's model for porous ductile metals, in: *Continuum Micromechanics*, P. Suquet, ed., CISM Courses and Lectures No. 377, Springer, pp. 61-130.

Gurson A.L. (1977). Continuum theory of ductile rupture by void nucleation and growth: Part I - Yield criteria and flow rules for porous ductile media, *ASME J. Engng. Materials Technol.*, **99**, 2-15.

Halphen B. and Nguyen Q.S. (1975). Sur les matériaux standards généralisés, *Journal de Mécanique*, **14**, 39-63, 1975 (in French).

Hill R. (1967). The essential structure of constitutive laws for metal composites and polycrystals, *J. Mech. Phys. Solids*, **15**, 79-95.

Leblond J.B., Perrin G. and Devaux J. (1994). Bifurcation effects in ductile metals with nonlocal damage, *ASME J. Appl. Mech.*, **61**, 236-242.

Mandel J. (1964). Contribution théorique à l'étude de l'écrouissage et des lois d'écoulement plastique, in: *Proceedings of the 11th International Congress on Applied Mechanics*, Springer, pp. 502-509 (in French).

Matsushima T., Chambon R. and Caillerie D. (2000). Second gradient models as a particular case of microstructured models: a large strain finite element analysis, *Comptes-Rendus Acad. Sc. Paris Série IIb*, **328**, 179-186.

Needleman A. and Tvergaard V. (1998). Dynamic crack growth in a nonlocal progressively cavitating solid, *Eur. J. Mech. A/Solids*, **17**, 421-438.

Nguyen Q.S. (1977). On the elastic plastic initial-boundary value problem and its numerical integration, *Int. J. Numer. Meth. Engng.*, **11**, 817-832.

Pijaudier-Cabot G. and Bazant Z.P. (1987). Nonlocal damage theory, *ASCE J. Engng. Mech.*, **113**, 1512-1533.

Shu J., King W. and Fleck N. (1999). Finite elements for materials with strain gradient effects, *Int. J. Numer. Methods Engng.*, **44**, 373-391.

Tvergaard V. (1981). Influence of voids on shear band instabilities under plane strain conditions, *Int. J. Fracture*, **17**, 389-407.

Tvergaard V. and Needleman A. (1984). Analysis of cup-cone fracture in a round tensile bar, *Acta Metall.*, **32**, 157-169.

Tvergaard V. and Needleman A. (1995). Effects of nonlocal damage in porous plastic solids, *Int. J. Solids Structures*, **32**, 1063-1077.

Tvergaard V. and Needleman A. (1997). Nonlocal effects on localization in a void-sheet, *Int. J. Solids Structures*, **34**, 2221-2238.

Rousselier G. and Mudry F. (1980). Etude de la rupture ductile de l'acier faiblement allié en Mn-Ni-Mo pour cuves de réacteurs à eau ordinaire sous pression, approvisionné sous la forme d'une débouchure de tubulure. Résultats du programme expérimental, *EdF Centre des Renardières Internal Report HT/PV D529 MAT/T43* (in French).

A Appendix : micromechanical foundations of the GLPD model

A.1 Basic principles - Definitions of the macroscopic strain rate and strain rate gradient

The derivation of the GLPD model is based on homogenization of some representative "elementary cell" $\mathcal{C}(\mathbf{X})$ of center $\mathbf{X}$ in some plastic porous medium subjected to conditions of *inhomogeneous* boundary strain rate. These boundary conditions read

$$v_i(\mathbf{x}) = A_{ij}x_j + \frac{1}{2}B_{ijk}x_jx_k \quad , \quad \forall \mathbf{x} \in \partial\mathcal{C}(\mathbf{X}) \tag{A.1}$$

where $\mathbf{v}(\mathbf{x})$ denotes the microscopic velocity, $\mathbf{A}$ a second-rank tensor which can be considered as symmetric since its antisymmetric part represents a mere rigid-body motion, and $\mathbf{B}$ a third-rank tensor which can obviously be considered as symmetric in its second and third indices.

The microscopic velocity field $\mathbf{v}(\mathbf{x})$ being extended arbitrarily over the voids enclosed in the elementary cell $\mathcal{C}(\mathbf{X})$, the *macroscopic strain rate* $\mathbf{D}(\mathbf{X})$ is defined as the average value $\langle\, \mathbf{d}(\mathbf{x}) \,\rangle_{\mathcal{C}(\mathbf{X})}$ of the microscopic Eulerian strain rate $\mathbf{d}(\mathbf{x}) \equiv \frac{1}{2}\left[\nabla_{\mathbf{x}}\mathbf{v}(\mathbf{x}) + (\nabla_{\mathbf{x}}\mathbf{v})^T(\mathbf{x})\right]$ over this cell. A simple calculation based on Green's formula then shows that

$$D_{ij}(\mathbf{X}) = A_{ij} + \frac{1}{2}\left(B_{ijk} + B_{jik}\right)X_k \quad \Rightarrow \quad D_{ij,k}(\mathbf{X}) = \frac{1}{2}\left(B_{ijk} + B_{jik}\right) \tag{A.2}$$

where the macroscopic position vector $\mathbf{X}$ is treated as a continuous variable. This equation shows in particular that the macroscopic strain rate $\mathbf{D}(\mathbf{X})$ and its gradient $\nabla_{\mathbf{X}}\mathbf{D}(\mathbf{X}) \equiv \nabla\mathbf{D}(\mathbf{X})$ are independent of the manner in which the field $\mathbf{v}(\mathbf{x})$ is extended over the voids.

Equation $(\text{A.2})_2$ may be inverted by writing it for the triplets $(i,\, j,\, k)$, $(j,\, k,\, i)$ and $(k,\, i,\, j)$ and combining the results using the symmetry of the tensor $\mathbf{B}$ in its last two indices. The result reads

$$B_{ijk} = D_{ij,k}(\mathbf{X}) - D_{jk,i}(\mathbf{X}) + D_{ki,j}(\mathbf{X}). \tag{A.3}$$

Thus, for given values of $\mathbf{D}(\mathbf{X})$ and $\nabla\mathbf{D}(\mathbf{X})$, equations $(\text{A.2})_1$ and (A.3) fully specify those of the tensors $\mathbf{A}$ and $\mathbf{B}$, and therefore the boundary conditions on the elementary cell.

A.2 Definition of macroscopic stresses and moments - The Hill-Mandel lemma

Let the microscopic Cauchy stress field $\boldsymbol{\sigma}(\mathbf{x})$ be defined as zero in the voids. (This preserves the statically admissible character of this field since the boundaries of the voids are traction-free). The second-rank tensor of *macroscopic stresses* $\boldsymbol{\Sigma}(\mathbf{X})$ and the third-rank tensor of *macroscopic moments* $\mathbf{M}(\mathbf{X})$ are then defined by the following formulae:

$$\begin{cases} \Sigma_{ij}(\mathbf{X}) & \equiv \langle\, \sigma_{ij}(\mathbf{x}) \,\rangle_{\mathcal{C}(\mathbf{X})} \\ M_{ijk}(\mathbf{X}) & \equiv \langle\, \sigma_{ij}(\mathbf{x})(x_k - X_k) \,\rangle_{\mathcal{C}(\mathbf{X})}. \end{cases} \tag{A.4}$$

Clearly, $\mathbf{\Sigma}(\mathbf{X})$ is symmetric and $\mathbf{M}(\mathbf{X})$ symmetric in its first two indices.

Using the principle of virtual work, the boundary conditions (A.1), Green's formula and equation $(A.2)_1$, one easily shows that

$$\langle\, \boldsymbol{\sigma}(\mathbf{x}) : \mathbf{d}(\mathbf{x}) \,\rangle_{\mathcal{C}(\mathbf{X})} = \Sigma_{ij}(\mathbf{X}) D_{ij}(\mathbf{X}) + M_{ijk}(\mathbf{X}) D_{ij,k}(\mathbf{X}) \equiv \mathbf{\Sigma}(\mathbf{X}) : \mathbf{D}(\mathbf{X}) + \mathbf{M}(\mathbf{X}) \vdots \nabla\mathbf{D}(\mathbf{X}). \tag{A.5}$$

This formula stands as an extension of the classical Hill-Mandel lemma for conditions of homogeneous boundary strain rate (Mandel (1964), Hill (1967)). Integrating it over the body Ω considered, one immediately gets the expression (2) of the text of the virtual power of internal forces $\mathcal{P}^{(i)}$.

The expression (3) of the text of the virtual power of external forces $\mathcal{P}^{(e)}$ is simply a postulate. It is based on the assumption that the boundary tractions do not vary quickly over $\partial\Omega$, so that no term proportional to the gradient of the macroscopic velocity need be introduced into this expression.

Indications of dependence of the tensors $\mathbf{D}$, $\nabla\mathbf{D}$, $\mathbf{\Sigma}$ and $\mathbf{M}$ upon $\mathbf{X}$ will be dropped from now on for simplicity.

A.3 Elimination of rigid-body motions - Restrictions on macroscopic moments

For any arbitrary third-rank tensor $\mathbf{T}$ symmetric in its first two indices, let $\overline{\mathbf{T}}$ denote the "deviator over non-symmetric indices" defined by

$$\overline{T}_{ijk} \equiv T_{ijk} - \frac{1}{4}\left(\delta_{ik} T_{jhh} + \delta_{jk} T_{ihh}\right). \tag{A.6}$$

The tensor $\overline{\mathbf{T}}$ is symmetric in its first two indices and "traceless" in the sense that

$$\overline{T}_{ijj} = 0; \tag{A.7}$$

it is zero if and only if $\mathbf{T}$ is of the form

$$T_{ijk} \equiv \delta_{ik} U_j + \delta_{jk} U_i \tag{A.8}$$

for some vector $\mathbf{U}$.

The derivation of the GLPD yield criterion is based on consideration of an elementary cell of the simplest possible shape, that is *spherical*, of radius b. It so happens that for such a cell, a macroscopic strain rate gradient $\nabla\mathbf{D}$ having a zero deviator $\overline{\nabla\mathbf{D}}$, that is of the form (A.8), represents a mere rigid-body motion of the cell. Indeed the tensor $\mathbf{B}$ is then of the form $B_{ijk} = 2\delta_{jk}U_i$ by equation (A.3) so that by equation (A.1), the microscopic velocity is of the form $v_i(\mathbf{x}) = \delta_{jk}U_i x_j x_k = b^2 U_i = Cst.$ on $\partial\mathcal{C}(\mathbf{X})$. The implication is that macroscopic strain rate gradients $\nabla\mathbf{D}$ of the form (A.8) must make no contribution in the virtual power of internal forces, that is, the inner product $\mathbf{M} \vdots \nabla\mathbf{D} = 2M_{ijj}U_i$ must be zero for all possible tensors of macroscopic moments. This implies that $M_{ijj} = 0$, which is equation (1) of the text.

This equation can also be derived directly from consideration of the equilibrium of the spherical cell. Indeed, let the origin of space be taken at the center of the cell and $\mathcal{S}(r)$ denote the sphere of radius r with center at the origin. Global equilibrium of this sphere implies that

$$0 = \int_{\partial\mathcal{S}(r)} \sigma_{ij}(\mathbf{x}) n_j(\mathbf{x})\, dS = \frac{1}{r} \int_{\partial\mathcal{S}(r)} \sigma_{ij}(\mathbf{x}) x_j\, dS \quad \Rightarrow \quad \int_{\partial\mathcal{S}(r)} \sigma_{ij}(\mathbf{x}) x_j\, dS = 0,$$

and equation (1) of the text follows from there through integration from $r = 0$ to $r = b$, using the definition $(A.4)_2$ of the tensor $\mathbf{M}$.

A.4 Limit-analysis for a rigid ideal-plastic material

The material is now assumed to be rigid ideal-plastic and obey the von Mises yield criterion (with flow stress σ_0) and the Prandtl-Reuss flow rule associated to this criterion through normality. For any traceless microscopic strain rate tensor $\mathbf{d}$, the microscopic plastic dissipation $\pi(\mathbf{d})$ is defined by the classical formula

$$\pi(\mathbf{d}) \equiv \sup_{\boldsymbol{\sigma},\, \sigma_{eq} \leq \sigma_0} \boldsymbol{\sigma} : \mathbf{d} = \sigma_0\, d_{eq} \tag{A.9}$$

where $\sigma_{eq} \equiv \left(\frac{3}{2}\boldsymbol{\sigma}' : \boldsymbol{\sigma}'\right)^{1/2}$ ($\boldsymbol{\sigma}'$: deviator of $\boldsymbol{\sigma}$) and $d_{eq} \equiv \left(\frac{2}{3}\mathbf{d} : \mathbf{d}\right)^{1/2}$ denote the von Mises equivalent microscopic stress and plastic strain rate. For any macroscopic tensors $\mathbf{D}$ (not necessarily traceless) and $\nabla\mathbf{D}$, the *macroscopic plastic dissipation* $\Pi(\mathbf{D}, \nabla\mathbf{D})$ is then defined as

$$\Pi(\mathbf{D}, \nabla\mathbf{D}) \equiv \inf \langle\, \pi[\mathbf{d}(\mathbf{x})] \,\rangle_{\mathcal{C}(\mathbf{x})} \tag{A.10}$$

where the infimum is taken over the space of incompressible microscopic velocity fields $\mathbf{v}(\mathbf{x})$ satisfying the boundary conditions with the prescribed values of $\mathbf{D}$ and $\nabla\mathbf{D}$.

Using the extended Hill-Mandel lemma (A.5), it is then easy to establish the following *inequality of macroscopic plastic dissipation*, applicable to any plastically admissible pair $(\boldsymbol{\Sigma}, \mathbf{M})$:

$$\boldsymbol{\Sigma} : \mathbf{D} + \mathbf{M} \vdots \nabla\mathbf{D} \leq \Pi(\mathbf{D}, \nabla\mathbf{D}) \quad , \quad \forall (\mathbf{D}, \nabla\mathbf{D}). \tag{A.11}$$

Thus the domain of plastically admissible pairs $(\boldsymbol{\Sigma}, \mathbf{M})$ lies in the intersection of the semi-spaces (depending on the parameters $\mathbf{D}$ and $\nabla\mathbf{D}$) $\boldsymbol{\Sigma} : \mathbf{D} + \mathbf{M} \vdots \nabla\mathbf{D} \leq \Pi(\mathbf{D}, \nabla\mathbf{D})$, and a classical result of limit-analysis asserts that it in fact coincides with this intersection. The boundary of this domain, that is the macroscopic yield locus, is the envelope of the hyperplanes (depending on $\mathbf{D}$ and $\nabla\mathbf{D}$) $\boldsymbol{\Sigma} : \mathbf{D} + \mathbf{M} \vdots \nabla\mathbf{D} = \Pi(\mathbf{D}, \nabla\mathbf{D})$ and is thus defined by the equations

$$\begin{cases} \boldsymbol{\Sigma} \;\; = \dfrac{\partial \Pi}{\partial \mathbf{D}}(\mathbf{D}, \nabla\mathbf{D}) \\ \mathbf{M} = \dfrac{\partial \Pi}{\partial (\nabla\mathbf{D})}(\mathbf{D}, \nabla\mathbf{D}) \end{cases} \tag{A.12}$$

where the tensors $\mathbf{D}$ and $\nabla\mathbf{D}$ act as parameters.

At the microscopic scale, Hill's principle of maximum plastic dissipation is satisfied: thus $(\boldsymbol{\sigma} - \boldsymbol{\sigma}^*) : \mathbf{d} \geq 0$ where $\boldsymbol{\sigma}$ and $\boldsymbol{\sigma}^*$ denote arbitrary plastically admissible microscopic

stress tensors and $\mathbf{d}$ the strain rate associated to $\boldsymbol{\sigma}$ through the microscopic flow rule. Using again the extended Hill-Mandel lemma (A.5), one gets from there the following macroscopic counterpart of Hill's principle:

$$(\boldsymbol{\Sigma} - \boldsymbol{\Sigma}^*) : \mathbf{D} + (\mathbf{M} - \mathbf{M}^*) \vdots \nabla\mathbf{D} \geq 0 \tag{A.13}$$

where $(\boldsymbol{\Sigma}, \mathbf{M})$ and $(\boldsymbol{\Sigma}^*, \mathbf{M}^*)$ represent arbitrary plastically admissible pairs and $(\mathbf{D}, \nabla\mathbf{D})$ the "generalized strain rate" associated to $(\boldsymbol{\Sigma}, \mathbf{M})$ through the macroscopic flow rule.

Following a classical reasoning, one concludes from there that the equation of the domain of plastically admissible pairs $(\boldsymbol{\Sigma}, \mathbf{M})$ being written in the form $\Phi(\boldsymbol{\Sigma}, \mathbf{M}) \leq 0$, the macroscopic flow rule reads

$$\left\{ \begin{array}{ll} D_{ij} & = H \dfrac{\partial \Phi}{\partial \Sigma_{ij}}(\boldsymbol{\Sigma}, \mathbf{M}) \\ D_{ij,k} & = H \dfrac{\partial \Phi}{\partial M_{ijk}}(\boldsymbol{\Sigma}, \mathbf{M}) + \delta_{ik} U_j + \delta_{jk} U_i \end{array} \right. , \quad H \left\{ \begin{array}{lll} = 0 & \text{if} & \Phi(\boldsymbol{\Sigma}, \mathbf{M}) < 0 \\ \geq 0 & \text{if} & \Phi(\boldsymbol{\Sigma}, \mathbf{M}) = 0 \end{array} \right. \tag{A.14}$$

where H (the *macroscopic plastic multiplier*) is an arbitrary scalar and $\mathbf{U}$ an arbitrary vector. The unusual extraneous term $\delta_{ik} U_j + \delta_{jk} U_i$ in equation $(A.14)_2$ arises from the fact that the tensors of macroscopic moments obey the constraint (1). Indeed it follows from this constraint and the definition (A.6) of the deviator $\overline{\mathbf{T}}$ that $(\mathbf{M} - \mathbf{M}^*) \vdots \nabla\mathbf{D} = (\mathbf{M} - \mathbf{M}^*) \vdots \overline{\nabla\mathbf{D}}$, so that inequality (A.13) does place restrictions upon the deviator $\overline{\nabla\mathbf{D}}$ of $\nabla\mathbf{D}$ but not upon its "orthogonal part" of the form $\delta_{ik} U_j + \delta_{jk} U_i$.

A.5 Approximate macroscopic yield criterion for a spherical elementary cell

An approximate overall yield criterion for a hollow sphere of center O, internal radius a, external radius b, porosity $f \equiv a^3/b^3$, subjected to boundary conditions of type (A.1), was derived by Gologanu *et al.* (1997) using the formalism presented above. We shall only present a brief sketch of their elaborate calculations.

Gologanu *et al.* (1997) first focussed on the case of a loading possessing a cylindrical symmetry about some radial direction OZ. They calculated some approximate value of the macroscopic plastic dissipation $\Pi(\mathbf{D}, \nabla\mathbf{D})$ by considering only four trial velocity fields, and then managed to eliminate the parameters $\mathbf{D}$ and $\nabla\mathbf{D}$ in the parametric equations (A.12) of the corresponding approximate macroscopic yield locus, so as to get its *explicit* equation. The result was the following "extended Gurson criterion":

$$\Phi(\boldsymbol{\Sigma}, \mathbf{M}) \equiv \frac{1}{\sigma_0^2} \left[(\Sigma_{ZZ} - \Sigma_{XX})^2 + \frac{Q^2}{b^2} \right] + 2f \cosh\left(\frac{3}{2} \frac{\Sigma_m}{\sigma_0} \right) - 1 - f^2 \leq 0. \tag{A.15}$$

In this expression $\Sigma_m \equiv \frac{1}{3} \operatorname{tr} \boldsymbol{\Sigma} = \frac{1}{3}(2\Sigma_{XX} + \Sigma_{ZZ})$ denotes the mean stress and Q^2 some quadratic form of the moment components M_{XXZ} and M_{ZZZ}.

Gologanu *et al.* (1997) then heuristically extended this expression to arbitrary macroscopic stress states by replacing $(\Sigma_{ZZ} - \Sigma_{XX})^2$ and Q^2 by quadratic invariants of the macroscopic

stress and moment tensors $\mathbf{\Sigma}$, $\mathbf{M}$. The result was equations (8), (10) and (11) of the text (with σ_0 and f instead of Σ and p).

A.6 Other elements of the model

The other elements of the model were derived by Gologanu *et al.* (1997) in a more heuristic way.

In order to account for elasticity, they first introduced the phenomenological hypothesis of additive decomposition of the macroscopic strain rate and strain rate gradient in the form (4).

They then derived an elasticity law of type (5), (7) from approximate elastic homogenization of a spherical cell, and transformed this elastic law into a hypoelastic one by heuristically replacing the strain tensor by the Eulerian elastic strain rate and the stress tensor by its Jaumann (objective) time-derivative [10]. (In fact a slight modification of Gologanu *et al.* (1997)'s hypoelasticity law is introduced in the present work in order to simplify the numerical implementation of the model; this modification is permissible in view of the minor role played by elasticity in problems of ductile rupture).

In order to account for the plastic behavior, the Gurson-like yield criterion derived as explained in Subsection A.5 was adopted with three modifications. First, (isotropic) strain hardening was introduced, following Gurson (1977), by retaining the yield criterion found for an imaginary ideal-plastic material but heuristically replacing σ_0 by some average value Σ of the heterogeneous yield stress in the real, hardenable material. Second, the porosity was multiplied by some empirical parameter q, as suggested by Tvergaard (1981) to bring the model predictions to closer agreement with the results of some micromechanical FE simulations. Third, the true porosity f was replaced by some fictitious, larger one f^* during coalescence, following Tvergaard and Needleman (1984), in order to account for the accelerated degradation of the material during this final stage of ductile damage.

The flow rule (A.14) derived from limit-analysis for a rigid-plastic material was assumed to remain applicable to an elastic-plastic material with the sole replacement of the strain rate $\mathbf{D}$ and its gradient $\nabla\mathbf{D}$ by their plastic parts $\mathbf{D}^p$, $(\nabla\mathbf{D})^p$.

Finally Gologanu *et al.* (1997) adopted the classical evolution equation (14) of the porosity resulting from approximate incompressibility of the metallic matrix. Also, in order to derive an evolution equation for the "average yield stress" Σ, they used Gurson (1977)'s suggestion to identify the plastic dissipation $(1-f)\Sigma\dot{E}$ in the fictitious "equivalent" ideal-plastic material, with uniform yield stress Σ, to the dissipation in the true, heterogeneous material. The presence of the extraneous term $\mathbf{M}\vdots(\nabla\mathbf{D})^p$ in the expression of the latter dissipation arose from the extended Hill-Mandel lemma (A.5).

[10] The expression $(6)_2$ of the Jaumann derivative of the third-rank tensor $\mathbf{M}$ is not classical but may easily be derived from the fact that is represents the time-derivative of $\mathbf{M}$ in the matter's comoving frame, which rotates with the velocity $\mathbf{\Omega}$.